High outcrossing rates in a self-compatible and highly aggregated host-generalist mistletoe

Manru Li, Yi Sui, Xuanni Wang, Zhanxia Ma, Yahuang Luo, Sasith Tharanga Aluthwattha, Doyle Mckey, Benoit Pujol, Jin Chen, Ling Zhang

High outcrossing rates in a self-compatible and highly aggregated host-generalist mistletoe

Manru Li[1,2,§], Yi Sui[1,2,§], Xuanni Wang[1,2], Zhanxia Ma[1,2], Yahuang Luo[1,2], Sasith Tharanga Aluthwattha[1], Doyle McKey[3], Benoit Pujol[4], Jin Chen[1] and Ling Zhang[1*]

[1] CAS Key Laboratory of Tropical Forest Ecology, Xishuangbanna Tropical Botanical Garden, Chinese Academy of Sciences, Mengla, Yunnan 666303, China, [2] University of Chinese Academy of Sciences, Beijing 100049, China, [3] CEFE, Univ Montpellier, CNRS, EPHE, IRD, Montpellier, France, [4] PSL Université Paris, EPHE-UPVD-CNRS, USR 3278 CRIOBE, Université de Perpignan, 52 Avenue Paul Alduy, CEDEX 9, 66860 Perpignan, France

[§]*These authors contributed equally to this work*

**For Correspondence. E-mail zhangl@xtbg.org.cn*

Running head: High outcrossing rate in a generalist mistletoe

Original Article

Abstract

Plants have evolved various strategies to avoid inbreeding, but the mass flowering displayed by many plants predisposes them to within-plant pollen movements and self-pollination. Mistletoes often aggregate at multiple spatial scales. Their bird pollinators often visit several flowers of the same individual and of others on the same host tree. We hypothesized that hermaphroditic mistletoes have self-incompatibility mechanisms that reduce or prevent selfing. Whether their spatial distribution, affected by host specificity, host distribution, and the behaviour of seed dispersers, influences their mating system and population genetic structure remains unclear. We studied how mating system and spatial distribution affect genetic structure in four populations of the host-generalist mistletoe *Dendrophthoe pentandra* in southwest- ern China using microsatellite markers and progeny arrays. We also characterized the fine-scale spatial genetic structure among 166 mistletoes from four host trees in one population. Prevalence and intensity of infection both appeared to vary among host species, strongly affecting the degree of aggregation. Host tree size had a strong effect on infection intensity. Surprisingly, manual pollination experiments indicated that *D. pentandra* is self-compatible, but genetic analyses revealed that outcrossing rates were higher than expected in all four populations (MLTR tm 0.83–1.20, Bayesian tm 0.772–0.952). Spatial genetic structure was associated with distance between host trees but not at shorter scales (within hosts). Our results demonstrate that the combination of bird pollination, bird-mediated seed dispersal, and post-dispersal processes result in outcrossing and maintain relatively high diversity in the presence of biparental

inbreeding, despite very high local densities and possible self-compatibility.

Key words: aggregation, bird pollination, genetic structure, hermaphroditic, mating system, self-compatibility

1|INTRODUCTION

Mating systems play a key role in the demographic and genetic dynamics of plant populations (Barrett & Harder, 2017). Mechanisms to avoid inbreeding have evolved in many plant species, as for example in hermaphroditic plants pollinated by animals transporting pollen between compatible plants (Barrett & Harder, 1996). This is because although selfing confers some advantages, for example, reproductive assurance and automatic transmission advantage, it also has detrimental effects, for example, discounting of pollen and ovules, and inbreeding depression (Charlesworth & Charlesworth, 1987; Husband & Schemske, 1996). Amongst the strategies that plants have evolved to avoid inbreeding, one can find floral characteristics such as heterostyly, physiological self-incompatibility, cryptic self-incompatibility (post pollination discrimination between self and outcross pollen), and spatial or temporal separation of male and female functions (herkogamy and dichogamy, respectively), mediated via the behaviour of pollinating animals (Charlesworth & Charlesworth, 1987; Cruzan & Barrett, 2016; Hiscock & McInnis, 2003). Parasitic plants are phylogenetically and ecologically diverse and have complex life histories that condition where potential mates are located and where parasite propagules are dispersed (Amico et al., 2014; Yule et al., 2016). Characterizing the mating system of parasitic plants can help us not only understand the re- productive ecology of the species, but also predict how the species' genetic structure may change when the habitat conditions change, via host switching, habitat fragmentation, or other causes.

Mistletoes, a group of aerial hemiparasitic plants, include about 1,600 species in five families in the order Santalales (Watson, 2020). They are keystone resources in forest and

woodland ecosystems, providing valuable food resources and nest sites for many vertebrates, mostly birds (Watson, 2001). They are highly dependent not only on host plants for water and minerals via their special root system, that is, haustoria, but also on biotic vectors for pollination and seed dispersal by animals attracted to their plentiful nectar and fleshy fruits (Aukema, 2003). Their interactions with pollinators may facilitate outcrossing, thereby affecting the mating system and the genetic structure of mistletoe populations (Amico et al., 2014). Some mistletoes possess specialized features that attract specialist vectors (e.g., flowerpeckers, Dicaeidae), such as the production of explosive flowers that are mostly opened by birds (Feehan, 1985; Ladley & Kelly, 1995). Furthermore, some mistletoes even produce flowers that mimic fruit colours in order to attract otherwise frugivorous pollinators, combined with fruiting times that overlap with sub- sequent blooming periods, with the result that a common vector is used for both seed and pollen dispersal (Davidar, 1983; Start, 2011; Watson, 2001). Dichogamy (protandry) facilitates sequential visits of birds to flowers in male and female phases, thereby favouring outcrossing and preventing selfing (e.g., Mathiasen et al., 2008; Pérez-Crespo et al., 2016). Previous studies indicated that individual mistletoes produce many flowers simultaneously and that pollinating birds may visit several hermaphroditic flowers of the same individual sequentially (Guerra et al., 2014). Thus, effective avoidance of selfing may require full or partial self-incompatibility, a contention supported by some studies (e.g., Gonzalez et al., 2007).

Another general characteristic of mistletoe species is their highly aggregated distribution at multiple spatial scales, that is, at host individual, host species, plot, local, and regional

scales (e.g., Luo et al., 2016; Morrill et al., 2017; Rist et al., 2011; Ward & Paton, 2007). In order to study the dynamic interaction of ecology and genetic structure in parasites (both plants and animals), specific parameters describing their spatial distribution have been adopted, such as infection prevalence, infection intensity, and the degree of aggregation (Aukema, 2004; Young & Young, 1998). For mistletoes, these parameters can be calculated for each host tree species and for all trees in a site, the two levels giving complementary information. For a host-generalist mistletoe, different host species vary in compatibility as potential hosts, that is, some host species may have high infection prevalence and intensity, whereas those of other species are rarely and only lightly parasitized (Luo et al., 2016). Different hosts may also differ in their resistance to mistletoe infections (Yan, 1993). Similarly, there may be great variation in infection intensity among individuals of the same host tree species, owing to differences in environment, for example, exposure to sunlight (Fontúrbel et al., 2017). Also, infection intensity is often positively correlated with host tree height, crown size, or diameter at breast height, because of the preference of frugivorous birds for tall perches and because older (generally larger) hosts accumulate mistletoes over time (Aukema & Martinez del Rio, 2002; Ndagurwa et al., 2012; Sreekar et al., 2016). Furthermore, individual trees may differ in their resistance to mistletoe infection, and an initial infection can increase the probability of reinfection (Aukema & Martinez del Rio, 2002).

Distribution patterns of mistletoes may influence fitness by effects on the mating system. Aggregated distribution of mistletoes in some host trees may result in higher levels of outcrossing, particularly for dioecious mistletoes (e.g., Yule & Bronstein, 2018), as dense

populations produce more flowers and larger floral displays and may facilitate attraction of mistletoes' pollinators (Caballero et al., 2013; Skorka & Wojcik, 2005; Yule & Bronstein, 2018). In self-compatible hermaphroditic mistletoe species, however, the effects of aggregated distributions on mating systems may be complex, depending on whether pollinators visit neighbouring plants within aggregations, and on whether these neighbouring plants are close relatives or not, which in turn depends on the movement patterns of seed-dispersing birds. If birds only disperse seeds at limited distances, a tree (or a group of neighbouring trees) may harbour genetically closely related mistletoes; if this is the case, movements of pollinators among aggregated plants could lead to high rates of biparental inbreeding, resulting in low genetic diversity and perhaps inbreeding depression. *Dendrophthoe pentandra*, a mistletoe with a broad host-plant range, is the most common mistletoe species in Xishuangbanna, southwestern China. In a previous study, Luo et al. (2016) reported that *D. pentandra* exhibited an aggregated distribution at a local scale, and different seed dispersers had different effects on the initial distribution template of mistletoes, determining small-scale patterns in the populations. In the present study, we combined data on the spatial distribution, the behaviour of pollinating birds, and the mating system, to disentangle factors shaping outcrossing rate and genetic structure of different populations. We tried to address the following specific questions: (1) What traits of trees affect density and dispersion patterns of mistletoes among individual trees? (2) What is the mating system of *D. pentandra* in the four populations studied? (3) Are the populations genetically structured at a fine spatial scale? (4) How does *D. pentandra* maintain outcrossing in these populations differing in density and level of aggregation?

|2 | MATERIALS AND METHODS

2.1 | Study species and sites

Dendrophthoe pentandra is a predominantly tropical mistletoe species that is common in southwestern China and Indochina (Qiu & Gilbert, 2004). In Xishuangbanna, it is the most commonly occurring mistletoe, where it parasitizes up to 361 host species belonging to 72 families and 224 genera (Xiao & Pu, 1988). This host-generalist mistletoe is hermaphroditic and its flowers require an external force, usually by pollinating birds, to open the mature corolla and expose anthers and stigmas (Start, 2011; M.R. Li, personal observation).

We conducted field observations and experiments at two sites over four years (2011–2014; Figure 1). The first site was in an area of Xishuangbanna Tropical Botanical Garden in Menglun County (ML; 21°45′N, 101°20′E; 580 m a.s.l.), where a wild vegetable collection was mixed with planted trees and some secondary forest. This site was dominated by *Citrus maxima* (Rutaceae) and *Mangifera indica* (Anacardiaceae), which were also the principal host species for *D. pentandra* at this site. The second site was ~70 km away in Jinghong County (JH; 22°00′N, 100°47′E; 550 m a.s.l.) where D. *pentandra* mostly

parasitizes *Syzygium szemaoense* (Myrtaceae), which is very abundant there. In 2014, we studied populations at two additional locations, also in Jinghong County: the wayside trees adjacent to natural forests and rubber plantations near Mengyang Nature Reserve (MY; 22°09′N, 100°53′E; 730 m a.s.l.) and the wayside trees in remnant patches of natural forest in Puwen town (PW; 22°28′N, 101°04′E; 830 m a.s.l.) (Figure 1).

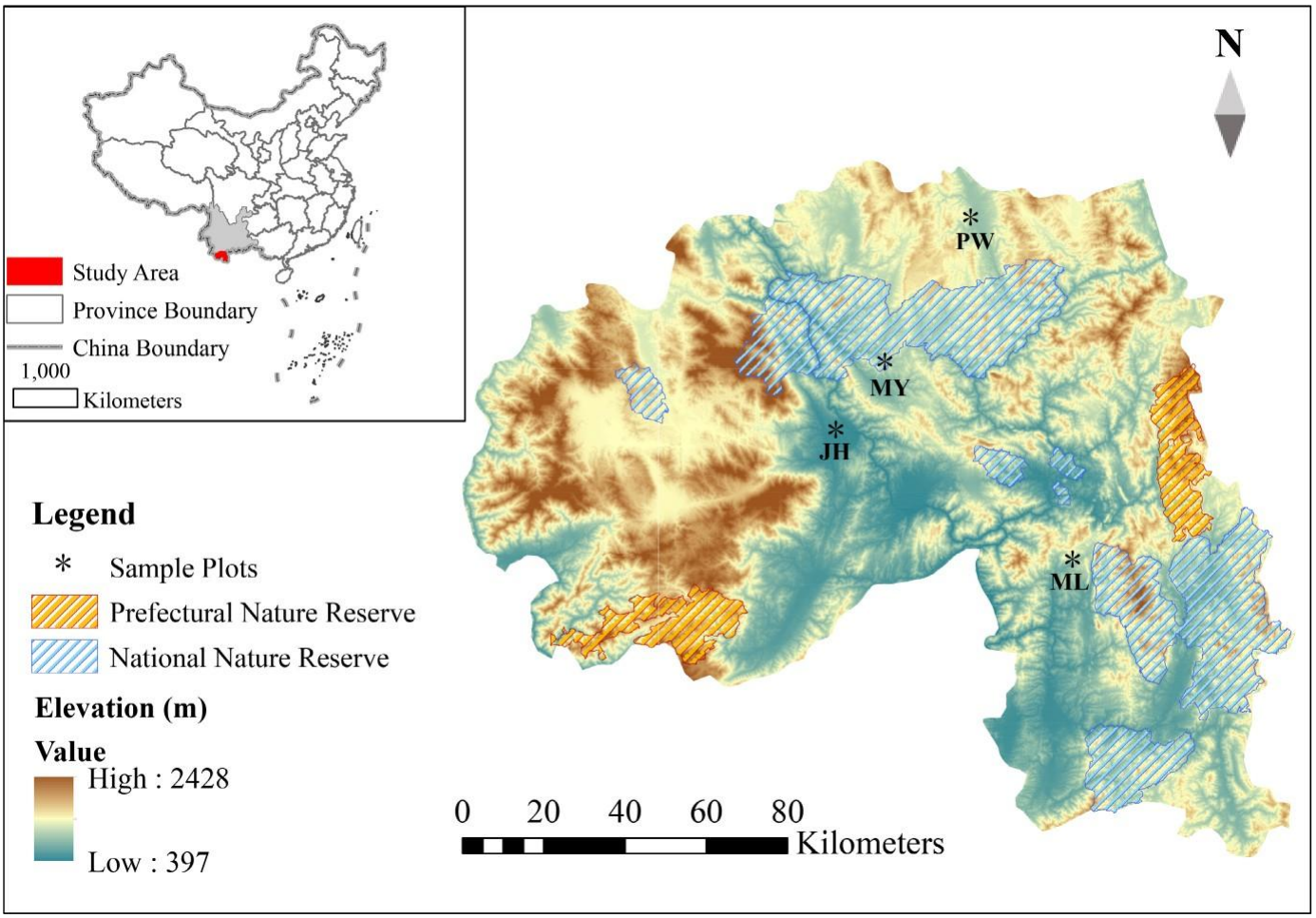

Figure 1. The locations of populations investigated in this study in Xishuangbanna, in southern Yunnan province, SW China. Base map, Yunnan provincial platform for common Geospatial information service (Number: Yun S[2017]048), https://www.ynmap.cn/; Terrain data, http://srtm.csi.cgiar.org/.

2.2 | Mistletoe infection patterns

We determined patterns of spatial distribution of mistletoes by plot survey in these four sites, totaling 13 plots (four plots in the ML site and three plots in each of the other three sites, each 20 × 20 m; plots in the same site were at least 100 m apart). All mistletoe individuals we counted possessed a distinct basal haustorium. While *D. pentandra* is among the species listed by Calvin and Wilson (2006) as potentially capable of forming ramets via fragmentation of epicortical roots, we observed no indication of such clonal growth. Within each plot, we recorded all individual trees (hosts and nonhosts) and counted all individuals of this mistletoe. The total number of trees in the four sites combined was 186 (72 in ML, 40 in MY; 32 in JH; 42 in PW). Because several different dimensions of tree size have been hypothesized to influence infection intensity, we recorded three size parameters: tree height, tree crown height (h), and tree crown diameter (d). We used the last two measurements to estimate crown volume. Following Frank (2010), each tree was treated as a cylinder, so that $v = \pi\ h\ d2/4$. Although a simplification, this estimate allows quantifying relative values of crown volume across trees. We then determined which tree species and which individual trees were infected by *D. pentandra*. Based on the field survey, we calculated the plot characteristics including species richness, abundances of all tree species, and tree crown volume. We also determined *D. pentandra* infection intensity for each tree (the number of mistletoe individuals on a given tree) and infection prevalence for each plot and population (the proportion of trees infected by at least one mistletoe individual; Aukema, 2004).

For each tree species represented by a sufficient number of individuals, we tested whether

infection prevalence was significantly different from that of the overall sample of trees, using binomial tests. The overall level of aggregation was determined by calculating the variance-to-mean ratio of mistletoe numbers per host individual (Young & Young, 1998), excluding uninfected individuals. We conducted a generalized linear mixed-effects model (GLMM) with distributions of Poisson family to test the effects of tree height on mistletoe infection intensity per crown volume. Random effects included host trees nested within each site in the model. Host tree height and number of mistletoes per cubic meter of crown volume were both log10-transformed before analysis.

2.3 | Floral biology

We observed flowering and fruiting phenology, measured pollen- ovule ratios, pollen viability, stigma receptivity, nectar secretion and sugar concentration to obtain data on some basic biological traits of *D. pentandra* at the ML population during 2011–2014. (1) We randomly selected one inflorescence from each of 30 plants and monitored the total number of flowers and the flowering du- ration of inflorescences. (2) Pollen grains and ovules of one flower from each of these 30 inflorescences were also counted. We used haemocytometers to estimate the number of pollen grains in each flower. As each flower contains only a single ovule and therefore produces one seed, we then calculated the mean pollen-ovule (P:O) ratio of the flowers. (3) We used 0.1% 3-(4,5-dimethylthiazol-2-yl)-2,5-diphenyl-tetrazolium bromide to test for the presence of dehydrogenase as an assay for pollen viability (Rodriguez-Riano & Dafni, 2000). To prevent insect visits, one

inflorescence from each of 10 different individuals was netted with a nylon net bag just prior to anthesis of the first flowers, and then we tested pollen vi- ability from one flower from each of these 10 inflorescences every 12 h over four days. The same assay was used to assess stigma receptivity (Dafni & Maues, 1998), using the same number of experimental flowers from the same plants. All tests were conducted under warm, sunny weather conditions. (4) We randomly selected one flower from each of four different inflorescences from each of nine study plants that were ~100 m apart (i.e., a total of 36 flowers), and bagged them with nylon net bags in the afternoon prior to anthesis. We examined the nectar secretion dynamics by repeatedly extracting nectar from these 36 flowers every 3 h from 08:00 h to 17:00 h in three successive days (28–30 March 2012). The nectar volume (μl) was measured with 10- and 20-μl SIGMA "micro-cap" calibrated capillary tubes (Sigma-Aldrich) and nectar sugar concentration (% mass sugar/total mass solution) was deter- mined with a hand-held, temperature-compensated refractometer (Eclipse, Bellingham and Stanley, Ltd.).

2.4 | Controlled pollination experiments

We conducted five pollination treatments on flowers from single inflorescences from 60 randomly selected individual *D. pentandra* plants in each of two populations (ML and JH) in 2014, in order to test whether plants are self-compatible and whether visitors are required for pollination (or whether, on the contrary, autonomous self-pollination can occur). These treatments (N = 60 inflorescences for each treatment in each of the two sites,

save for exceptions noted below) were (1) natural open pollination (N), (2) hand selfed pollination (S), (3) hand outcrossed pollination (HC), (4) hand geitonogamous pollination (moving pollen to different flowers on the same plant; HG), and (5) bagging (autonomous autogamy, B). For each treatment, except natural open pollination, we bagged inflorescences on each plant before anthesis, in order to prevent pollinator access. In addition, two days prior to anthesis, we emasculated the flowers to prevent prior self-pollination for treatments (3) and (4). We carried out artificial cross-pollinations by hand, using mixed pollen that was collected from one inflorescence of each of 10 plants at least 100 m apart. The total number of flowers for each treatment in each site varied from 201 to 409, except for treatments (3) and (4). Owing to the technical difficulties related to bud emasculation in this species, smaller numbers of flowers received these treatments (hand cross-pollination: 143 [in 39 inflorescences] in ML, 74 [21] in JH; hand geitonogamous pollination: 120 [32] in ML, 100 [26] in JH). Fruits were collected one month later and fruit set (the proportion of all flowers that set fruit from each inflorescence) was calculated. No apomixis treatment was included in this study because emasculated and bagged flowers do not set fruit (Luo, 2012).

Based on the non-normality of fruit set (Shapiro-Wilk normality test, $p < .001$), we fitted binomial generalized linear models (GLM) to determine the effects of pollination treatments, populations, and interactions between treatments and populations on fruit set. Following the result of GLM, we then calculated fruit set (mean ± SD) across all treatments and used the Kruskal-Wallis H test (Wilcoxon Rank aum tests) to test for differences in fruit set among populations and treatments. All analyses were carried out

using R version 4.0.3 (R Core Team, 2020).

2.5 | Flower visitors and pollinators

Observations were made continuously from 08:00 h to 18:00 h using video cameras (Sony HDR-XR150E). For each plant, we thus recorded 10 h of video per day over 3 days. Recording was con- ducted on a total of 27 plants (nine plants in each of two years in ML, nine plants in one year in JH). Our sample of video recordings was thus 180 h in ML (in 2012, 2013) and 90 h in JH (in 2013). We noted the total number of flower visitors on each plant and the number of flowers visited. We classed visitors in one of two groups (visitors and pollinators) based on their behaviour and their assessed likelihood of acting as pollinators. Birds simply observed on inflorescences were considered visitors, whereas birds that consistently contacted both anthers and stigmas and had pollen grains deposited on their bodies were considered pollinators. Before each day's observations, the number of ripe buds and open flowers on each plant within a selected field of vision were recorded (Weston et al., 2012). The size of this focal area varied among individual plants and was delimited in order to achieve a clear field of vision including numerous ripe floral buds and newly opened flowers. We photographed all types of floral visitors and consulted bird experts to identify species we did not know. Furthermore, we conducted additional video recordings in the ML population to explore whether frequency of bird visits varied with infection intensity.

2.6 | Mating system, genetic diversity, and analysis of genetic differentiation

From each of the four populations, we genotyped 16–23 adult plants (total of 76) for 13 simple sequence repeat (SSR) loci specifically developed for this study (GenBank accession numbers: KT264232, KT264233, KT264234, KT264235, KT264236, KT264237, KT264238, KT264239, KT264240, KT264241, KT264242, KT264243, and KT264244; Table S1). We also genotyped 10–12 seeds, randomly sampled, from each of the adult plants (a total of 829 seeds). We extracted total genomic DNA from the dried leaf tissue of mature plants or fresh seeds (offspring) using a modified cetyl trimethyl ammonium protocol (Doyle, 1991). Quantification of DNA was carried out using a SmartSpec Plus Spectrophotometer (Bio-Rad, Hercules). Working stocks of DNA were then prepared on the basis of these estimates and stored in 0.1× TE buffer. All the SSR fragments were amplified individually via standard PCR in 20 μl reaction mixtures that contained 30–50 ng genomic DNA template, 0.6 μM each primer, 7.5 μl 2× Taq PCR MasterMix (Tiangen; 0.1 U Taq polymerase/μl, 0.5 mM each dNTP, 20 mM Tris-HCl [pH = 8.3], and 100 mM KCl, 3 mM MgCl2). PCR amplifications were conducted in a Bio-Rad thermal cycler, as follows: 95°C for 3 min followed by 30–36 cycles at 94°C for 30 s, with the annealing temperature optimized for each specific primer (see Table S1) for 30 s, 72°C for 60 s, and a final extension step at 72°C for 7 min. The fluorescence-labelled PCR products were denatured and analysed on an ABI PRISM 3730XL DNA sequencer (Applied Biosystems). The genotypes were scored using GeneMapper software version 3.7 (Applied Biosystems) and the data were rechecked manually to reduce scoring errors.

Population genetic differentiation was estimated by Wright's FST (Weir & Cockerham,

1984) calculated among populations on the basis of the 76 mature plants. Calculation was done by analysing molecular variance (AMOVA) with GenAlEx version 6.501 (Peakall & Smouse, 2012). The genetic diversity of each of the four populations (JH, ML, MY, & PW) was estimated by the unbiased expected heterozygosity index Hnb (Nei, 1978), and by the number of alleles per locus (Na), the number of effective alleles (Ne), Shannon's information index (I), the observed and expected heterozygosity (HO, HE), and the fixation index (F) based on the 76 mature plants. We tested for departure from the expected Hardy-Weinberg equilibrium under random mating by estimating Wright's FIS in each population. FIS was considered statistically significant if its 95% confidence interval (calculated by conducting 10,000 bootstrap calculations) did not over- lap zero. Genetic diversity and FIS were calculated using GENETIX (Belkhir et al., 1996–2004).

We characterized the mating system of each population by estimating the probability of outcrossing, and related parameters, on the basis of progeny arrays in each population. We used the multi- locus analysis software MLTR3.4 (Ritland, 2002), which is applicable to codominant markers. To do this, we used the Newton-Raphson method, with default parameter settings (t = 0.9, Fm = 0.9, rt = 0.1, rp = 0.1) and 95% confidence interval based on bootstrap values (10,000 iterations with resampling at the family level) for the total of 76 parents and their 829 progeny. Parameters calculated include the multilocus outcrossing rate (tm), single-locus outcrossing rate (ts), outcrossing rate among related individuals (tm − ts), multilocus correlation of paternity (rpm), inbreeding coefficient of maternal mature plants (Fm), and expected inbreeding coefficient (Fe).

Because the MLTR method can be affected by genotyping errors, which could be frequent

for microsatellite data, we also characterized the mating system by using a Bayesian approach following the framework proposed by Chybicki et al. (2019) that uses computer simulations in order to reduce genotyping errors and other possible biases. We used quedo version 0.6, compiled using the GFortran compiler, designed by Chybicki et al. (2019) to estimate effects of ecological variables on outcrossing rates. Estimation procedure is based on a hierarchical Bayesian approach and uses the reversible jump Markov Chain Monte Carlo algorithm. This novel Bayesian statistical method addresses explicitly the variation of outcrossing rates (t), genotyping errors, such as allele dropout (e1) and allele misclassification (e2), genetic structure between populations and divergence rates (F), while selecting the best regression model to estimate effects of ecological variables (b) on outcrossing rates under both single- and multilocus scenarios.

We selected three prior values for outcrossing rates (0.25, 0.5 and 0.8; same across families, tested separately), while other prior values were adopted from Chybicki et al. (2019), that is, prior value for population divergence rates 0.01 (same across locations), prior value for allele dropout 0.025 (same across markers), prior value for allele mistyping 0.01 (same across markers). We tested the above three prior outcrossing rates in both multilocus and single-locus scenarios, estimating genotyping errors as well as ignoring incompatibilities. Results are given from the best models of each of the two scenarios. Outcrossing rates were log-transformed for normality and then a one-way ANOVA was performed to compare their variation among populations. We then conducted a Wilcoxon rank sum test for pairwise comparisons. We investigated four ecological variables for their contribution to explaining outcrossing rates: tree height (b1), tree crown volume (b2), infection intensity

(b3), and mistletoe individuals per crown volume (b4), which are at the population level. Variables were standardized and all values were Z-transformed before the analyses.

We used recommended settings for the MCMC algorithm (Chybicki et al., 2019). We set number of initial MCMC iterations to 10,000. During the initial stage, the program runs the saturated regression model in order to adjust proposal distributions for parameters. Another 10,000 iterations were used for pilot tuning of proposal distributions. We ran 100,000 iterations for sampling, while every 50th update of a parameter, in total 2000, from the posterior distribution were used for final estimates. For each parameter, we computed the frequency of true model selection. Additionally, we computed the coverage of the 95% highest posterior density interval (HPD95%, estimated as the shortest range that included 95% of sorted MCMC samples).

2.7 | Fine-scale spatial genetic structure

To quantify the fine-scale spatial genetic structure within trees, we performed spatial autocorrelation analysis at the level of mistletoe individuals and host trees. First, we selected four neighbouring host trees of *Mangifera indica* in the ML population. We mapped the location of each host tree using the host tree trunk as the centre, fixed the x-axis with due east, divided the area underneath the tree crown into four quadrants, and then recorded the spatial position on the tree of each mistletoe individual according to its position (X, Y, Z) in three-dimensional space. The calculation of the spatial distance was performed in R version 4.0.3 (R Core Team, 2020). The distance be- tween each pair of mistletoes on the four trees was calculated using the distance function between two points

in three-dimensional space sqrt((x1 − x2)2+(y1 − y2)2+(z1 − z2)2). Pairwise distances ranged from 0.32 m (different individuals in the same host tree) to 20.96 m (between an individual in tree 1 and an individual in tree 3).

Second, we used a resampling approach to study spatial auto-correlation at the level of mistletoe individuals. Significance tests were conducted by comparing the observed distribution with the simulated distribution. For each plot, geographic locations were randomly permuted 10,000 times to test if the observed mean kinship coefficients were different from those expected from a simulated distribution for each distance class. The simulated distribution can be obtained by assuming that all genotypes are distributed randomly in space. Spatial genetic structure was analysed using the SPAGEDI version 1.3 software (Hardy & Vekemans, 2002). Kinship coefficients (Fij) between each two samples were calculated following the method of Loiselle et al. (1995). Multilocus kinship coefficients per distance interval within tree were computed for 14 distance classes at 0.5 m intervals. For all samples from four host trees, we estimated mean kinship coefficients among all pairs of individuals within each of 25 distance classes at 1.0 m intervals. The significance of these kinship coefficients was tested using 10,000 permutations.

The autocorrelation coefficient is defined by rij, which shows the genetic correlation between the ith and jth individuals. The coefficient rij is a scale-free measure of genetic similarity between pairs of individuals, and is closely related to “kinship” (Loiselle et al., 1995). This analysis was performed using the GenAlEx software (Peakall & Smouse, 2012). We used 9999 permutations with a bootstrap resampling procedure run 10,000 times to estimate the 95% confidence interval. We used two very similar approaches to evaluate

spatial autocorrelation in SPAGEDI and GenAlEx but we show only the results of the GenAlEx approach because they gave similar results.

Genetic structure of all mistletoe individuals in all four host trees was explored using a discriminant analysis of principal components (DAPC). DAPC summarizes the genetic variability using linear combinations of the alleles as variables. It maximizes the variability be- tween groups and minimizes the within-group variance (Jombart & Balloux, 2010). Coefficients of the alleles used in the linear combination are called loadings, while the synthetic variables are themselves referred to as discriminant functions. DAPC provides group membership probabilities that can be seen as proximities of individuals to different clusters. We performed the dapc command in adegenet version 1.3-6 (Jombart, 2008) on R version 4.0.3.

3 | RESULTS

3.1 | Spatial distribution pattern of mistletoes

Tree height had a significant positive effect on mistletoe infection intensity (defined as the number of mistletoe individuals in a host tree; uninfected individuals excluded) per crown volume of tree ($Rm2 = 0.15$, $p = .003$, $n = 98$) (Figure 2). For all host trees in the four populations combined, the shortest trees had the lowest infection intensity while the highest infection intensity was found in the tallest trees (Figure 2). Degree of mistletoe

aggregation was thus partly explained by variation in tree size. The plot characteristics and infection patterns in the four populations are shown in Table 1.

Table 1. The plot characteristics and infection patterns of *Dendrophthoe pentandra* in the study plots in four populations

	Populations			
Parameter	JH	ML	MY	PW
Plotcharacteristics				
Number of plots	3	4	3	3
Tree species richness	3.3 ± 0.9	5.0 ± 1.7	5.0 ± 1.0	4.0 ± 0.6
Total number of trees	10.7 ± 1.2	18.0 ± 2.0	13.3 ± 1.8	14.0 ± 1.5
Tree height (m)	9.5 ± 0.7	6.1 ± 0.5	12.2 ± 0.7	10.6 ± 0.3
Tree crown volume (m3)	897.64 ± 138.03	448.00 ± 140.04	737.67 ± 78.44	564.71 ± 89.47
Infection pattern				
Number of infected tree species	1.7 ± 0.3	2.0 ± 0.4	2.3 ± 0.3	2.0 ± 0.6
Number of infected individuals	6.0 ± 0.6	10.5 ± 2.9	6.7 ± 0.0	6.7 ± 1.5
Infection intensity	23.7 ± 8.3	3.4 ± 0.7	15.3 ± 2.0	9.7 ± 3.7
Infection prevalence (%)	52.22 ± 7.79	54.75 ± 15.04	47.62 ± 2.38	55.00 ± 22.91
Variance/mean ratio of infection intensity	32.13 ± 13.31	2.72 ± 0.15	14.47 ± 1.19	11.22 ± 5.76
Mistletoe individuals per crown volume	0.033 ± 0.007	0.017 ± 0.003	0.041 ± 0.008	0.043 ± 0.014

Note: “Infection prevalence” is the proportion of all trees in the plot that bore at least one individual mistletoe, “infection intensity” is the number of mistletoe plants on each host tree. Variance/mean ratio of infection intensity takes only infected individuals into account.

All results are shown as mean ± SE.

JH, Jinghong; ML, Menglun; MY, Mengyang; PW, Puwen.

However, size was not the only trait of trees that influenced infection intensity and aggregation at the levels of plot and site. The relationship between height and infection intensity appeared to vary among tree species well-represented in the overall sample. Infection prevalence also differed among common tree species. In two species, infection prevalence was significantly higher than in the overall tree assemblage (98 of 186 [0.53]): *Mangifera indica* (25 of 31 individuals infected, $p < .001$) and *Grevillea robusta* (22/23, $p < .001$). In contrast, infection prevalence in one species was significantly lower than in the overall assemblage: *Cassia siamea* (9/40, $p < .001$) (Table 2).

Table 2. Infection prevalence and intensity, and degree of aggregation, of *Dendrophthoe pentandra* on the five most common host species in the four sites

Host species	Total number	Number infected	Infection prevalence	Mean infection intensity for infected trees	Variance/mean ratio of infection intensity (including infected and uninfected trees)	p-value
Citrus maxima	18	11	0.61	2.5	1.98	.48
Mangifera indica	31	25	0.81	4.5	2.96	<.001***
Syzygium szemaoense	24	14	0.58	25.8	41.67	.54

Cassia siamea	40	9	0.225	2.3	3.32	<.001***
C. siamea in MY	16	1	0.063	7.0	7.0	<.001***
C. siamea in PW	24	8	0.33	1.8	1.63	<.001***
Grevillea robusta	23	22	0.96	17.8	5.06	<.001***
G. robusta in MY	14	13	0.93	19.3	5.41	<.001***
G. robusta in PW	9	9	1.00	15.7	4.85	<.001***

Note: For each species, a binomial test examined whether the proportion of infected individuals was significantly different (lower or higher) from that for all trees regardless of species (98 of 186 [0.53]).

MY, Mengyang; PW, Puwen.

***p < .001.

3.2 | Floral biology

The anthesis of *D. pentandra* flowers could occur at any time during the day and each flower lasted 3–4 days. Timing of anthesis was found to be reliably indicated by swelling of the corolla tube and a change in its colour from green to yellow (Figure S1). Plants

produced 3–14 (6.6 ± 0.8, mean ± SE, N = 30) flowers per inflorescence, and the inflorescences generally flowered for 3–11 days (7.4 ± 0.7, N = 30) and produced 1–4 flowers per day. Flowering occurred mainly from early February to mid-April, with sporadic production of inflorescences until early May. In addition, anthers and stigmas within flowers were very close, and individual flowers produced 960–12,240 pollen grains (6184 ± 651, N = 30) and only a single ovule. Therefore, the mean pollen-ovule ratio was 6,184:1. Pollen viability was high (~73%) when flowers opened and remained high (~61%) on the second day, but decreased rapidly on the third day (Figure S2A). Meanwhile, stigmas were already partially receptive when flowers reached anthesis, and their receptivity increased quickly, reaching a maximum on the second day, remaining high on the third day, and declining gradually on the fourth day (Figure S2A). There is thus a brief period in the development of each flower when pollen is viable and the stigma is receptive, allowing self-pollination. *Dendrophthoe pentandra* also produced nectar continuously during the first day of anthesis. Average volume and concentration of nectar were both highest immediately after anthesis and decreased gradually thereafter. On the second day, the nectar volume of most flowers fell to zero, but a few flowers continued to secrete nectar until the third day (see Figure S2B).

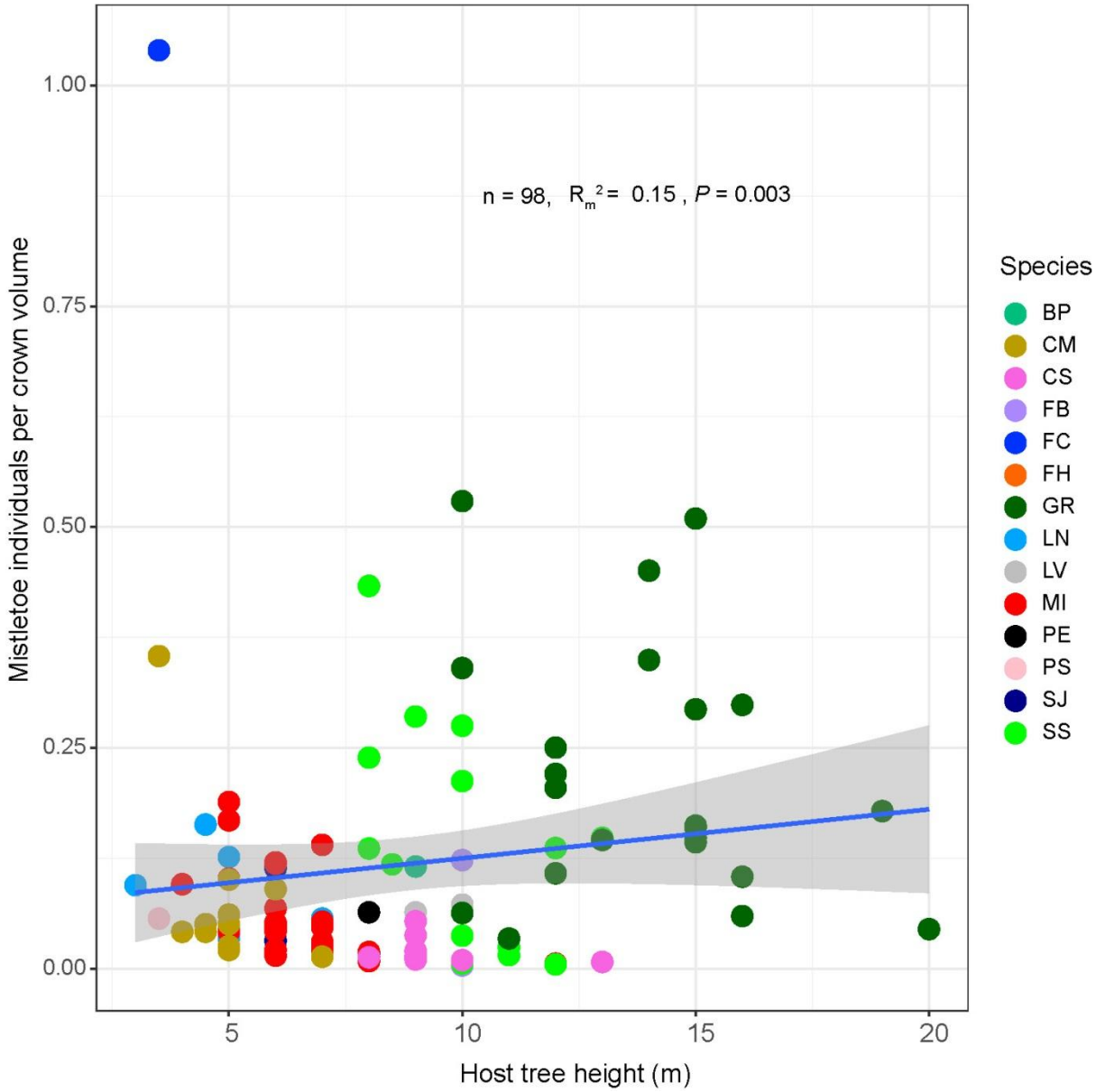

Figure 2. Effect of host tree height on mistletoe infection intensity per crown volume of tree. Different colours indicate different tree species. BP, *Broussonetiapa pyrifera*; CM, *Citrus maxima*; CS, *Cassia siamea*; FB, *Ficus benjamina*; FC, *Fraxinus chinensis*; FH, *Ficus hispida*; GR, *Grevillea robusta*; LN, *Lucuma nervosa*; LV, *Lagerstroemia villosa*; MI, *Mangifera indica*; PE, *Phyllanthus emblica*; PS, *Prunus salicina*; SJ, *Syzygium jambos*; SS, *Syzygium szemaoense*. Uninfected individuals were excluded from the analysis.

3.3 | Controlled pollination experiments

Although 60 inflorescences were included in each treatment, the sample sizes were reduced one month later, when fruits reached maturity, owing to damage from birds, humans, and bad weather. For the two populations combined, the GLM analysis indicated that treatments influenced the fruit set of mistletoe ($p < .05$) (Table S2), and the fruit set with bagged inflorescences (2.3 ± 6.0%, N = 52 inflorescences [plants], n = 678 flowers, $p < .001$) was lower than in other treatments (N: 30.2 ± 35.0%, N = 71, n = 736; S: 40.7 ± 33.4%, N = 56, n = 446; HC: 32.0 ± 31.6%, N = 60, n = 431; HG: 19.4 ± 26.1%, N = 58, n = 447). Meanwhile, we found significant differences be- tween the two populations (ML and JH) ($F_{1, 287} = 7.56$, $p = .006$) and among the five treatments ($F_{4, 287} = 18.46$, $p < .001$). Figure 3 illustrates the broad variation between pollination treatments and populations. In both populations, fruit set in hand outcrossed-pollinated was higher than in hand geitonogamous-pollinated inflorescences but this trend was not statistically significant. For each of these treatments, there was no significant difference between populations in fruit set, except for the hand self-pollination treatment. In ML, fruit set in self-pollinated flowers was significantly higher than that in other hand-pollinated treatments in the same population. Collectively, these data show that *D. pentandra* is self-compatible and that under our experimental conditions fruit set under self- pollination is sometimes comparable to that under open-pollination and hand-outcrossing.

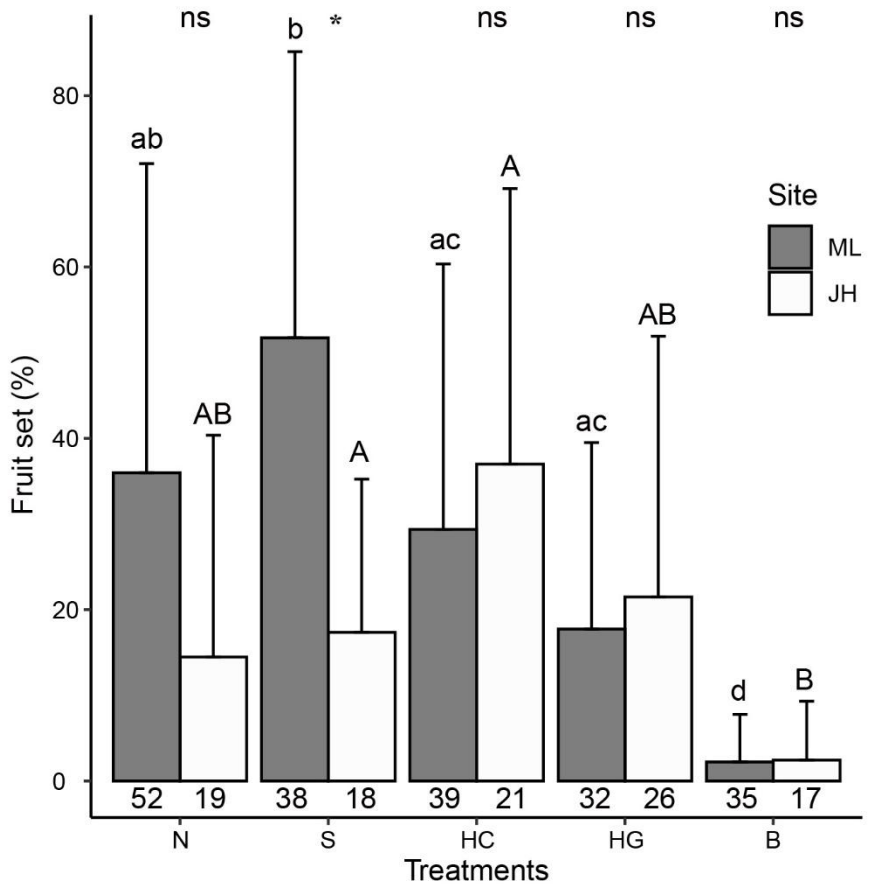

Figure 3. Effects of pollination treatment and of site on fruit set of *Dendrophthoe pentandra* in Menglun (ML) and Jinghong (JH) study sites. Fruit sets are expressed as mean percentages (±SD), and sample sizes (number of inflorescences) are given at the base of each column. N, natural open pollination; S, hand self-pollination; HG, hand geitonogamy; HC, hand cross-pollination; B, bagging. Different letters indicate significantly different means (Wilcoxon rank sum tests) at $p < .05$, the capital and lowercase letters represent differences among different treatments at ML and JH sites, the top row represents comparisons between the same treatments among ML and JH sites.

3.4 | Flower visitors and pollinators

In this study, seven passerine bird species belonging to six families were observed on mistletoes. Of these, one (*Orthotomus sutorius*, Common Tailorbird) did not visit flowers of mistletoe. A total of 111 visits (95 visits in ML, 16 visits in JH) were recorded during flowering (Figure 4). *Zosterops* simplex (Swinhoe's White-eye) was dominant in both sites. In ML site, six bird species, Z. simplex (39 visits, 221 flowers), *Pycnonotus jocosus* (Red-whiskered Bulbul; 26 visits, 163 flowers), *Arachnothera longirostra* (Little Spiderhunter; 15 visits, 76 flowers), *Aethopyga siparaja* (Crimson Sunbird; 9 visits, 96 flowers), *Dicaeum minullum* (Plain Flowerpecker; 5 visits, 28 flowers), *Phylloscopus inornatus* (Yellow-browed Warbler; 1 visit, 1 flower). In JH site, three bird species were recorded visiting mistletoe flowers: *Z. simplex* (8 visits, 26 flowers), *P. jocosus* (4 visits, 27 flowers), and *D. minullum* (4 visits, 6 flowers). In both sites, we observed that birds stayed at one mistletoe for long periods, tending to move from one flower to another on the same plant before moving to another plant. This behaviour pattern should promote geitonogamy.

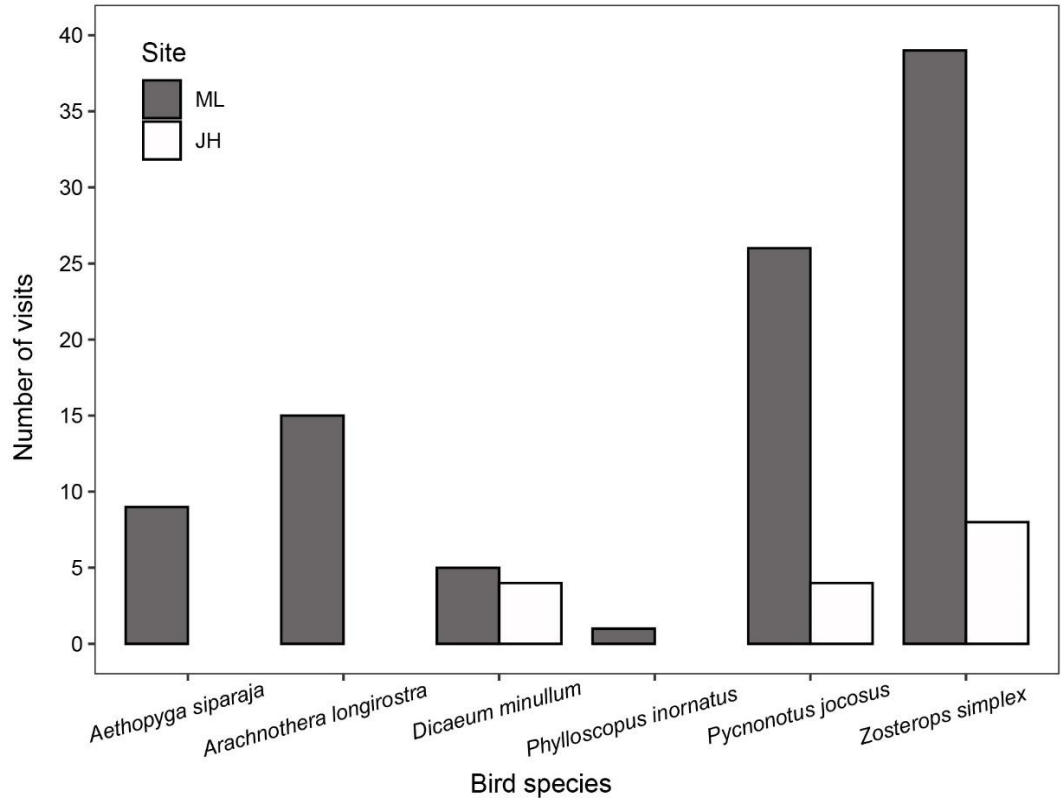

Figure 4. Number of visits by different bird species of *Dendrophthoe pentandra* in the Menglun (ML) and Jinghong (JH) populations.

3.5 | Genetic diversity and population differentiation

Within-population genetic diversity was moderate and showed no marked differences among populations (Table 3). Nei's unbiased index of genetic diversity varied from 0.45 to 0.51 in the different populations (Table 3). FIS estimated for each of the four populations showed no departure from Hardy-Weinberg proportions (none was significantly different from zero, Table 3), a result indicating random mating. Values of fixation indices estimated among populations by the AMOVA showed there was significant population genetic differentiation. The FST indicated that allelic frequencies differed by 32% (p = .001) among

populations (Table S3). The relatively high global FIT (38%, p = .001) indicates that the global pool of individual genes results from the combination of alleles whose frequencies differ among populations. The low but significant global FIS (9%, p = .002) indicates the absence of within-population substructure in geno- typic frequencies under random mating and therefore the absence of either an excess or a deficit of heterozygotes within populations, in contrast with the expectation that biparental inbreeding would result from related parents mating more often than expected under random mating assumptions. Although estimation of FST is highly reliable here because it was estimated while taking into account other types of subpopulation and total gene pools, the other Wright F-statistics estimated by AMOVA (Table S4) should be interpreted with caution.

Table 3. Genetic diversity measures from 13 microsatellite loci for 76 adult *Dendrophthoe pentandra* plants from four populations

	Populations				
Parameter	JH	ML	MY	PW	Mean for the four populations
Number of plants	16	23	17	20	19.0 ± 0.4
Number of alleles (Na)	4.0 ± 0.5	4.2 ± 0.7	3.9 ± 0.7	3.5 ± 0.5	3.9 ± 0.3
Effective number of alleles (Ne)	2.3 ± 0.3	2.3 ± 0.3	2.4 ± 0.5	2.3 ± 0.2	2.3 ± 0.2
Shannon's information index (I)	0.9 ± 0.1	0.9 ± 0.2	0.8 ± 0.2	0.9 ± 0.1	0.9 ± 0.1
Observed heterozygosity (HO)	0.447 ± 0.062	0.425 ± 0.068	0.376 ± 0.084	0.483 ± 0.081	0.433 ± 0.036
Expected heterozygosity (HE)	0.471 ± 0.058	0.448 ± 0.07	0.431 ± 0.081	0.496 ± 0.067	0.462 ± 0.034
Fixation index (F)	0.030 ± 0.061	0.039 ± 0.045	0.154 ± 0.086	0.046 ± 0.077	0.067 ± 0.034
Unbiased expected heterozygosity index (Hnb)	0.486 ± 0.216	0.458 ± 0.259	0.445 ± 0.299	0.509 ± 0.247	

Hardy-Weinberg equilibrium (Wright's FIS)	0.083	0.074	0.159	0.052

Note: Data are expressed as means ± SD.

JH, Jinghong; ML, Menglun; MY, Mengyang; PW, Puwen.

3.6 | Mating system: high outcrossing rate in all four populations

From the analysis using MLTR, the probabilities for outcrossing to occur in the four populations, estimated by their multilocus out- crossing rates (tm), ranged from 0.83 to 1.20. The outcrossing rates were very high in the four populations and could not be distinguished from 100% in three of the four populations (Table 4). Only in the JH population did the 95% confidence intervals of multilocus outcrossing rates not overlap with one. Even in this population, the upper limit of CIs was 0.95, which is very close to one. CIs for the different populations mostly overlapped with one another, which suggests that outcrossing rates may therefore not be considered different among populations. Only JH versus ML, and JH versus PW, could be reliably considered significantly different based on their 95% CIs estimated by using MLTR. Outcrossing rates among genetically related mistletoe individuals (tm − ts) were relatively high, ranging from 0.34 to 0.75 (Table 4), implying that biparental inbreeding probably occurred to some extent in all four populations, and especially in PW.

Table 4. Estimated mating system parameters from the analysis using MLTR on the basis of 13 loci for four populations of *Dendrophthoe pentandra*

Population	N (family/ progeny)	tm	ts	tm − ts	rpm	Fm	Fe
JH	16/173	0.83 (0.71; 0.95)	0.49 (0.37; 0.61)	0.34 (0.26;0.42)	0.40 (0.26;0.54)	0.014 (-0.06;0.09)	0.074
ML	23/256	1.20 (1.04; 1.36)	0.68 (0.60; 0.76)	0.52 (0.36;0.68)	0.38 (0.22;0.54)	0.082 (0.01; 0.16)	0.020
MY	17/180	0.91 (0.68; 1.12)	0.51 (0.41; 0.61)	0.40 (0.20;0.60)	0.71 (0.51; 0.91)	0.134 (-0.00;0.27)	0.038
PW	20/220	1.20 (1.00; 1.40)	0.46 (0.40; 0.52)	0.75 (0.55;0.95)	0.99 (0.95; 1.03)	0.082 (-0.01;0.18)	0.050

Note: JH, Jinghong; ML, Menglun; MY, Mengyang; PW, Puwen. tm, multilocus outcrossing rate; ts, single-locus outcrossing rate; tm − ts, outcrossing rate among relatives; rpm, multilocus correlation of paternity; Fm, inbreeding coefficient of maternal mature plants; Fe, expected inbreeding coefficient. Data are expressed as means; values in parentheses represent 95% confidence intervals based on 10,000 bootstraps.

Our results from the Bayesian analyses, which are expected to be more precise because several potential biases are corrected for (see methods), also showed high outcrossing rates in the four populations. Average multilocus outcrossing rates (tm) ranged from 0.772 to 0.952 (Table 5). A one-way ANOVA revealed that there was a significant difference in mean outcrossing rates (tm) between at least two populations ($F(3, 72) = 20.91$, $p = .000$). In Wilcoxon rank sum tests of pairwise comparisons, we found that outcrossing rate in the

JH population (0.772) was significantly lower than that in populations PW (0.952, p = .0003) and ML (0.943, p = .0007) but not different from that in population MY (0.824, p = .653). Outcrossing rate in population MY was significantly lower than in populations ML (p = .0007) and PW (p = .0004). Outcrossing rates in populations PW and ML were not significantly different (p = .6699). p-values were adjusted with Holm correction. Table 5 shows the outcrossing rates estimated in each population under both single-locus and multi- locus scenarios, given with HPD intervals.

Table 5. Outcrossing rates (t) and divergence rates (F) of the four studied populations under single-locus and multilocus scenarios

		Single-locus		Multi-locus	
parameter	Site	Mean	HPD $_{95\%}$	Mean	HPD $_{95\%}$
t_1	JH	0.679	0.5332; 0.8211	0.772	0.5797; 0.9245
t_2	ML	0.887	0.7658; 0.9805	0.943	0.8338; 0.9972
t_3	MY	0.679	0.5272; 0.8251	0.824	0.8338; 0.9972
t_4	PW	0.874	0.7528; 0.9759	0.952	0.8481; 0.9986
F_1	JH	0.2935	0.2335; 0.3349	0.2951	0.2333; 0.3430
F_2	ML	0.2827	0.2035; 0.3317	0.2833	0.2047; 0.3373
F_3	MY	0.2904	0.2273; 0.3362	0.2928	0.2203; 0.3401
F_4	PW	0.3207	0.2725; 0.3852	0.3256	0.2731; 0.3975
F_k		0.2997	0.2554; 0.3520	0.3005	0.2471; 0.3479

Note: Fk: mean of gamma prior distribution for divergence rates. JH, Jinghong; ML, Menglun; MY, Mengyang; PW, Puwen.

In the multilocus scenario, the 12 most probable models had a cumulative probability of approximately 0.95. The models with the highest and second highest posterior probabilities

(Pr = 0.276 and 0.273, respectively) included the same two predictor variables, namely, tree crown volume and infection intensity as in the single- locus scenario (Tables S5 and S6). In the single-locus scenario, among sixteen regression models the 10 most probable models had a cumulative probability of approximately 0.95 (Figure S3). The model with the highest posterior probability (Pr = 0.386) included two predictor variables (Tables S5 and S6). The second most probable model, with a posterior probability of 0.354, included only tree crown volume as the predictor variable. When tested under different initial t values, the two most probable models included tree crown volume (negative effect on outcrossing rate), infection intensity (positive effect), or both, further indicating the possible importance of these two variables in affecting outcrossing rates. In most cases, however, only the effect of tree crown volume was significant (see Figure S3, Tables S5 and S6).

The Bayesian model and the MCMC simulation method also pro- vided estimates for gene pool divergence rates (Fk) and genotyping error rates. Under the single-locus scenario, divergence rates were between 0.256 and 0.352, with a mean divergence rate of 0.300. ML had the lowest divergence rates (0.283), while PW had the highest divergence rates (0.321). The multilocus scenario produced similar results (Table 5). Regarding genotyping error rates, all markers revealed estimates of random allele mistyping close to zero (Table S7). Per-locus rate of allele misclassification was highly correlated with the frequencies of parent–offspring incompatibility ($r_{Pearson} = 0.93$, $p < .0001$). However, per-locus estimates of allele dropout frequency did not show any correlation with the frequencies of parent– offspring incompatibility ($r_{Pearson} = 0.31$, $p = .301$).

3.7 | Fine-scale spatial genetic structure

The four trees harboured a total of 166 mistletoes, with 55, 35, 49 and 27 individuals, in host trees 1, 2, 3, and 4, respectively (Figure 5). We found no spatial autocorrelation of genotypes within each of the four trees (Figure 5). In tree 1 at the 6-m distance class and in tree 4 at the 4.5-m distance class (Figure 5), genotypes were less related than at other distance classes. The 95% confidence intervals of the autocorrelation coefficients overlapped zero at all distance classes. The global autocorrelogram at the scale of the four trees showed that there was some spatial autocorrelation at this broader scale, with positive spatial autocorrelation at the 12-m distance class and negative autocorrelation at the 25-m distance class (Figure 5), which corresponds to more relatedness within trees than between trees. Thus we detected the presence of spatial genetic structure at the scale of the distribution of different trees but not at the scale of a given tree. The first two principal components of DAPC that were plotted to obtain scatter plots provided a direct visual assessment of between-group structures. The hierarchical structure is visible in Figure 5, where three groups of genetically closer clusters can be identified (mistletoes in trees 1, 2, 3 and 4), although there was some overlap between clusters.

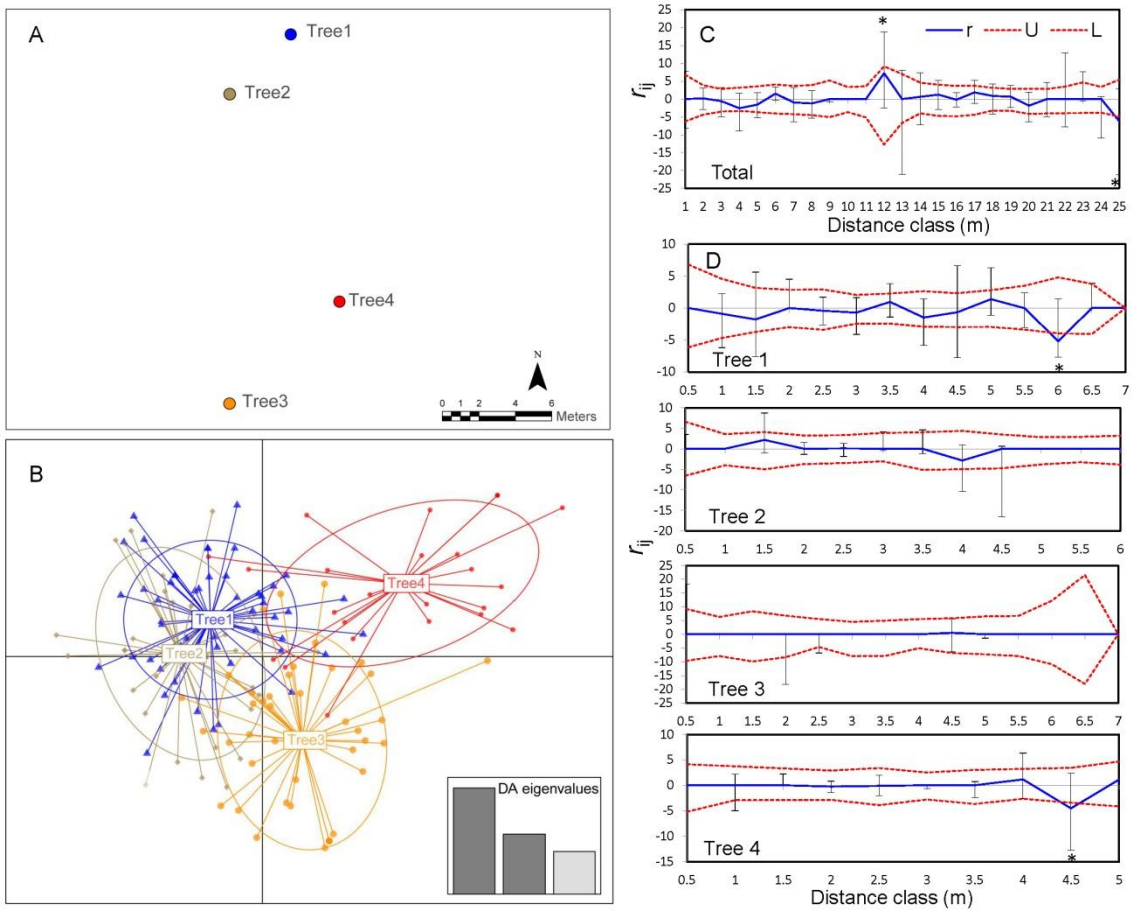

Figure 5. (a) Locations of the four host trees in the Menglun (ML) population from which individuals of *Dendrophthoe pentandra* were sampled, (b) scatter plots of discriminant analysis of principal components (DAPC), (c) the dynamic change of the average autocorrelation coefficient rij between pairs of individual mistletoes in the four sampled host trees with the change of geographic distance and (d) average autocorrelation coefficient rij between pairs of individual mistletoes in the four sampled host trees as a function of the geographical distance between them. (b) In the scatter plot using different host trees as priors, mistletoe individuals in different host trees are represented as different clusters. Clusters are shown in different colours and inertia ellipses, while dots represent mistletoe individuals. The 95% inertial ellipses around each cluster represent the variance of the two first principal components of the DAPC; Inset shows the histogram of

discriminant analysis (DA) eigenvalues. (c, d) Dashed lines represent upper and lower limits of the 95% confidence intervals determined by permutation.

4 | DISCUSSION

Our hand-pollination experiment indicated that the plant is self- compatible. We further observed the bird visitors were moving from one flower to another on the same mistletoe individual before moving to another individual, a pattern that could be expected to result in geitonogamy. However, all four populations examined showed high outcrossing rates. The Bayesian analysis revealed some variation in outcrossing rates among populations, and indicated a weak trend towards lower outcrossing rates in populations characterized by larger tree crown volume. However, the relationship is between population-level means of both outcrossing rate and tree crown volume, and should be interpreted with caution. Furthermore, we found no spatial genetic structure within a given host tree but there was some structure among host trees. The combination of reproductive-ecology and population-genetic approaches suggests that the nature of mechanisms promoting outcrossing in this mistletoe could be more complicated than assumed.

As expected for this host generalist, host range was broad, and there was great variation among tree species in infection prevalence and intensity (and of variation in intensity). Our data do not permit conclusions about causes of the marked variation in infection intensity among tree species and among conspecific individual trees. However, we did observe that in general, infection intensity increased with host tree size (e.g., height and crown volume;

see Figure 2). This correlation can have several causes. First, as the size of the host tree is generally related to its age, larger trees may simply have had more time to accumulate mistletoes (Overton, 1994). Second, larger trees have larger surface area to receive seeds (Martinez del Rio et al., 1996). Third, the birds that eat mistletoe fruits, and at the same time deposit more mistletoe seeds, often prefer to visit tall trees, and the tops of smaller trees (Aukema & Martinez del Rio, 2002). Fourth, establishment of mistletoe seedlings is often greatest in the sunniest parts of tree crowns and on stems of small to intermediate diameter, which are most numerous on tall trees and in the tops of trees (Norton & Ladley, 1998; Sargent, 1995). Finally, the greater the number of mistletoes in a tree, the more likely it is that the tree will attract the birds that eat mistletoe fruits and thus receive more seeds (Luo et al., 2016; Martinez del Rio et al., 1995), resulting in in- creased aggregation within some host trees but not in others. Initial infections might also weaken the tree's resistance against further infections (Aukema & Martinez del Rio, 2002).

In the mating model, MLTR handles all parent–offspring incompatibilities as missing data (the “blind correction” approach), which may lead to underestimation of selfing rates. Parent–offspring genotypic incompatibilities are often caused by genotyping errors. To avoid such underestimation of selfing rates, we considered possible genotyping errors, that is, mistyping (including null alleles) and allelic dropout in the Bayesian analyses with MCMC simulations. In all analyses, genetic substructuring was taken into account to avoid bias. We found that genotypic mother-offspring incompatibility rates were very low (close to zero) in both observed and simulated results. Nevertheless, multi- and single-locus outcrossing rates, and the difference between these two, are considered the most

fundamental descriptors of the plant mating system. Therefore, we ran all the simulations and analyses for both single- and multilocus scenarios. We found that differences between them were minor.

Dendrophthoe pentandra is self-compatible, as determined by controlled pollination experiments. It was thus surprising to find that the range of aggregation recorded in these populations had only a relatively small influence on outcrossing rate, which was high in all studied populations. The Bayesian analysis suggested a small negative effect of tree crown volume on outcrossing rate. It is also interesting to note that all four *D. pentandra* populations exhibited non-negligible levels of biparental inbreeding—outcrossing events between genetically partially related individuals—with particularly high values in the PW population (Table 4). In fact, self-compatibility is frequent in the Loranthaceae while autonomous selfing is rather rare, and outbreeding is considered to predominate (Aizen, 2005; Azpeitia & Lara, 2006). In *D. pentandra*, several floral traits may facilitate intrafloral self-pollination, such as hermaphroditism, the close proximity of anthers and stigmas within flowers, and anther dehiscence before flower opening (i.e., protandry). In addition, the behaviour of pollinators might facilitate intrafloral and interfloral (geitonogamous) selfing because they often spend prolonged periods within a single mistletoe. Thus, delayed selfing could provide reproductive assurance in this mistletoe while allowing outcrossing when mates are not limiting, as shown in other studies (e.g., Shirk & Hamrick, 2014).

Biparental inbreeding can also reflect reproductive assurance to some extent in a population in which the effective number of pollen donors is limited. Clustered mistletoe

flowers on a given host tree probably reduce the need for bird pollinators to fly widely (e.g., Stanton et al., 2009). Large clusters of flowers would also lead to local abundance of fruits, reducing the need for frugivores to fly widely. Inbreeding might thus be increased by frequent within-host seed dispersal by foraging birds (Stanton et al., 2009). Meanwhile, the flowers of *D. pentandra* secrete nectar continuously during the first day of anthesis and the tepals of the corolla tube require birds to open the flowers for pollination, a feature (explosive flowering) that has been best studied in African Loranthaceae (Feehan, 1985; Kirkup, 1998) and that is thought to be an adaptive strategy for specialized pollination by birds (Feehan, 1985). Bird grooming behaviour is associated with high outcrossing in bird-pollinated plants such as Banksia (Proteaceae) (Krauss et al., 2009). These traits of flowers and of birds might partly explain the high outcrossing rates observed here. Another possible factor explaining high outcrossing rates is cryptic self-incompatibility, which is functionally analogous to delayed selfing as it allows plants to preferentially outcross (Bowman, 1987; Cruzan & Barrett, 1996). If the ability of the species to discriminate self versus outcrossed pollen during post-pollination processes is sufficiently strong, mixed pollination can result in exclusively outcrossed seed despite a high rate of self-pollination (Cruzan & Barrett, 2016).

Outcrossing rates can fluctuate from year to year, and both spatial and temporal variation in mating patterns is well known in many other flowering plants (Pettengill & Moeller, 2012). It is possible that the outcrossing rate measured in a single year may not reflect the actual mating system of the population over several years. Fruit set may also vary between sites and years (M.R. Li, unpublished data), perhaps reflecting variation in pollination services.

Continuous nectar secretion by flowers during the first day of anthesis, and asynchronous flowering, may help attract bird pollinators, contributing to a high outcrossing rate even if pollinator abundance is locally or temporarily low. High outcrossing may also increase the infection success of mistletoe. In an experiment using controlled pollination, Gonzalez et al. (2007) showed that germination and radicle elongation were both enhanced in outcrossed seeds of *Tristerix aphyllus* compared to inbred seeds, resulting in a significant increase in the probability of establishment. One might speculate that the high outcrossing rate in *D. pentandra* populations can be attributed to aggregation, to greater attraction of birds promoting cross-pollination, and to the fact that neighbouring parental plants are not necessarily closely related, a fact perhaps explained by post-seed dispersal processes in this mistletoe, that is, extremely low rates of seedling survival and establishment (Luo et al., 2016).

Genetic diversity and its spatial structure are impacted by the life-history traits of plants, the processes of gene dispersal via pol- len and seeds, and the distribution patterns they generate. Mating system and seed dispersal are the main predictors of population differentiation (Hamrick & Godt, 1997; Nybom & Bartish, 2000). Owing to the clumped distribution of plants at small local scales, we expected that each of the four *D. pentandra* populations investigated in the present study would contain only a subset of the genetic variation present in the full sample. As expected, mistletoe populations were genetically differentiated from one another and exhibited moderate levels of genetic diversity and events of partial biparental inbreeding, indicating that aggregated mistletoe plants on a given host tree are sometimes related. Studies of two other mistletoe species have reported

similar or lower levels of genetic variability. For example, Jerome and Ford (2002) used AFLP markers to detect genetic diversity of *Arceuthobium americanum* (HT = 0.238, FST = 0.286), and Mejnartowicz (2006) used isozymes to study *Viscum album* (HO = 0.252, HE = 0.292, FST = 0.277). The higher degree of population genetic differentiation among the *D. pentandra* populations may be the result of habitat fragmentation, as reported in studies of other plants (e.g., Ewers & Didham, 2006; Potts et al., 2010).

Our findings on the spatial genetic structure of mistletoe plants imply that there is some spatial autocorrelation of genotypes at the scale of the plot of four host trees but a lack of such autocorrelation on any given host tree (Figure 5). This is in line with the findings on reproductive ecology presented above, in relation to the mating sys- tem. Although higher in selfing species, spatial autocorrelation is logically also increased by biparental inbreeding and limited pollen and/ or seed dispersal, and is inversely related to the population density (Vekemans & Hardy, 2004). *Dendrophthoe pentandra* is heavily dependent on many birds for pollination and seed dispersal. Foraging birds tend to remain on the same individual and forage among all the flowers and fruits of the same plant, and within the short flying distance of the specialized frugivorous bird *Dicaeum minullum* (Luo et al., 2016). Although birds may disperse a large number of seeds in each dropping that possibly originate from the same host trees, previous studies indicated that high mortality occurs afterwards and that only one seedling from each dropping finally establishes (Luo et al., 2016). Collectively, these aspects of mistletoe reproductive ecology are supported by our population-genetic findings at within- tree, plot and regional spatial scales.

Conclusions

Dendrophthoe pentandra exhibits a high level of outcrossing, despite self-compatibility. The species' dependence on birds for pollination, its aggregated distribution, and the mixing of genotypes resulting from seed dispersal by several bird species, allow it to maintain high outcrossing rates within moderately genetically diverse populations characterized by the spatial autocorrelation of genotypes at the scale of a plot of host trees and some biparental inbreeding. Although infection intensity and mistletoe density varied among populations, the outcrossing rate was always quite high. Overall, our results suggest that some mechanism of delayed selfing (per- haps cryptic self-incompatibility) provides reproductive assurance while allowing outcrossing when mates are not limiting. Our results show the interest of combining a wide range of reproductive and molecular ecology findings to characterize the mating system and its consequences for diversity, especially in self-compatible species, in particular when the capacity for selfing does not translate into frequent self-pollination.

AUTHOR CONTRIBUTIONS

Yi Sui and Ling Zhang designed the research; Yi Sui, Xuanni Wang, Yahuang Luo, Manru Li, and Ling Zhang collected samples and generated the data; Manru Li, Yi Sui, Zhanxia Ma, Yahuang Luo, Sasith Tharanga Aluthwattha and Benoit Pujol performed the analyses; Manru Li and Ling Zhang wrote the manuscript; Doyle McKey, Benoit Pujol, and Jin Chen commented on the research and on the manuscript, and all authors critically revised the manuscript.

ACKNOWLEDGEMENTS

We are very grateful to Mr Qiaoshun Li, Mr Shuyin Huang, and Mr Jianmin Gan of Xishuangbanna Tropical Botanical Garden (XTBG) for field assistance, to Professors Ruichang Quan and Xiaodong Yang of XTBG and Daniel Schoen of McGill University, Canada, for their constructive discussion and comments, and to Mr Jianbo Yang from the Center for Mountain Futures, Kunming Institute of Botany, Chinese Academy of Sciences, for constructing the study site map. The molecular laboratory work was conducted at the Germplasm Bank of Wild Species, Kunming Institute of Botany, Chinese Academy of Sciences, Kunming, Yunnan 650201, China. This study was sup- ported by the National Natural Science Foundation of China (grants 31670393 and 31170406).

CONFLICT OF INTEREST

The authors have declared no conflict of interest for this article.

DATA AVAILABILITY STATEMENT

DNA sequences have been deposited in the NCBI Nucleotide Database (GenBank accession nos. from KT264232 to KT264244). Data on flower lifetime, fruit set, nectar volume, sugar concentration, pollen viability, stigma receptivity, pollen-ovule ratio, visiting birds, host and nonhost characteristics, spatial locations, SSR markers for detecting mating system with MLTR and for quantifying effects of ecological variables on outcrossing with Bayesian analysis, and on spatial genetic structure of *Dendrophthoe pentandra* populations

are available from the Dryad Digital Repository: https://doi. org/10.5061/dryad.5dv41ns82.

ORCID

Manru Li https://orcid.org/0000-0002-0989-7278

Sasith Tharanga Aluthwattha https://orcid. org/0000-0002-9973-8165

Doyle McKey https://orcid.org/0000-0002-7271-901X

Benoit Pujol https://orcid.org/0000-0001-9703-6760

Ling Zhang https://orcid.org/0000-0002-0676-6221

REFERENCES

Aizen, M. A. (2005). Breeding system of *Tristerix corymbosus* (Loranthaceae), a winter-flowering mistletoe from the southern Andes. *Australian Journal of Botany*, *53*(4), 357–361. https://doi.org/10.1071/bt04088

Amico, G. C., Vidal-Russell, R., Aizen, M. A., & Nickrent, D. (2014). Genetic diversity and population structure of the mistletoe *Tristerix corymbosus* (Loranthaceae). *Plant Systematics and Evolution*, *300* (1), 153–162. https://doi.org/10.1007/s00606-013-0867-x

Aukema, J. E. (2003). Vectors, viscin, and Viscaceae: mistletoes as parasites, mutualists, and resources. *Frontiers in Ecology and the Environment*, *1*(4), 212–219. https://doi.org/10.1890/1540-9295(2003)001[0212:vvavma]2.0.co;2

Aukema, J. E. (2004). Distribution and dispersal of desert mistletoe is scale-dependent, hierarchically nested. *Ecography*, *27*(2), 137–144. https://doi.org/10.1111/j.0906-7590.2004.03640.x

Aukema, J. E., & Martinez del Rio, C. (2002). Variation in mistletoe seed deposition: effects of intra- and inter specific host characteristics. *Ecography*, *25*(2), 139–144. https://doi.org/10.1034/j.1600-0587.2002.250202.x

Azpeitia, F., & Lara, C. (2006). Reproductive biology and pollination of the parasitic plant *Psittacanthus calyculatus* (Loranthaceae) in central Mexico. *Journal of the Torrey Botanical Society*, *133*(3), 429–438. https://doi.org/10.3159/1095-5674(2006)133[429Rbapot]2.0.Co;2

Barrett, S. C. H., & Harder, L. D. (1996). Ecology and evolution of plant mating. *Trends in Ecology & Evolution*, *11*(2), 73–79. https://doi.org/10.1016/0169-5347(96)81046-9

Barrett, S. C. H., & Harder, L. D. (2017). The ecology of mating and its evolutionary

consequences in seed plants. *Annual Review of Ecology, Evolution, and Systematics*, *48*, 135–157. https://doi.org/10.1146/annurev-ecolsys-110316023021

Belkhir, K., Borsa, P., Chikhi, L., Raufaste, N., & Bonhomme, F. 1996-2004. GENETIX 4.05, logiciel sous Windows TM pour la génétique des populations. Laboratoire Génome, Populations, Interactions, CNRS UMR 5000, Université de Montpellier II ed, Montpellier, France.https://kimura.univ-montp2.fr/genetix/

Bowman, R. N. (1987). Cryptic self-incompatibility and the breeding system of *Clarkia unguiculata* (Onagraceae). *American Journal of Botany*, *74*(4), 471–476. https://doi.org/10.1002/j.1537-2197.1987.tb08667.x

Caballero, P., Ossa, C. G., Gonzales, W. L., Gonzalez-Browne, C., Astorga, G., Murua, M. M., & Medel, R. (2013). Testing non-additive effects of nectar-robbing ants and hummingbird pollination on the reproductive success of a parasitic plant. *Plant Ecology*, *214*(4), 633-640. https://doi.org/10.1007/s11258-013-0195-9

Calvin, C. L., & Wilson, C. A. (2006). Comparative morphology of epicortical roots in Old and New World Loranthaceae with reference to root types, origin, patterns of longitudinal extension and potential for clonal growth. *Flora*, *201*(1), 51–64. https://doi.org/10.1016/j.flora.2005.03.001

Charlesworth, D., & Charlesworth, B. (1987). Inbreeding depression and its evolutionary consequences. *Annual Review of Ecology and Systematics*, *18*, 237–268. https://doi.org/10.1146/annurev.es.18.110187.001321

Chybicki, I. J., Iszkuło, G., & Suszka, J. (2019). Bayesian quantification of ecological determinants of outcrossing in natural plant populations: Computer simulations and the case study of biparental inbreeding in English yew. *Molecular Ecology*, *28*, 4077–4096. https://doi.org/10.1111/mec.15195

Cruzan, M. B., & Barrett, S. C. H. (1996). Postpollination mechanisms influencing mating patterns and fecundity: An example from *Eichhornia paniculata*. *The American Naturalist*, *147*(4), 576–598. https://doi.org/10.1086/285867

Cruzan, M. B., & Barrett, S. C. H. (2016). Postpollination discrimination between self and outcross pollen covaries with the mating system of a self-compatible flowering plant. *American Journal of Botany*, *18*(3), 568–576. https://doi.org/10.3732/ajb.1500139

Dafni, A., & Maues, M. M. (1998). A rapid and simple procedure to determine stigma receptivity. *Sexual Plant Reproduction*, *11*(3), 177–180. https://doi.org/10.1007/s004970050138

Davidar, P. (1983). Similarity between flowers and fruits in some flowerpecker pollinated mistletoes. *Biotropica*,*15*(1), 32–37. https://doi.org/10.2307/2387995

Doyle, J. (1991). DNA protocols for plants-CATB total DNA isolation. In: Hewitt, G.M., & Johnston, A. (Eds.), *Molecular Techniques in Taxonomy*. Berlin, Germany: Springer.

Ewers, R. M., & Didham, R. K. (2006). Confounding factors in the detection of species responses to habitat fragmentation. *Biological Reviews*, *81*(1), 117–142. https://doi.org/10.1017/S1464793105006949

Feehan, J. (1985). Explosive flower opening in ornithophily: a study of pollination mechanisms in some Central African Loranthaceae. *Botanical Journal of the Linnean Society*, *90*, 129-144.

Fontúrbel, F. E., Salazar, D. A., & Medel, R. (2017). Increased resource availability prevents

the disruption of key ecological interactions in disturbed habitats. *Ecosphere*, *8*(4), e01768. https://doi.org/10.1002/ecs2.1768

Frank, E.F. (2010). Crown volume estimates. Eastern Native Tree Society. 1–29. Accessed at: https://docplayer.net/21475600-Crown-volume-estimates-edward-forrest-frank-december-10-2010-eastern-native-tree-society.html

Gonzalez, W. L., Suarez, L. H., & Medel, R. (2007). Outcrossing increases infection success in the holoparasitic mistletoe *Tristerix aphyllus* (Loranthaceae). *Evolutionary Ecology*, *21*(2), 173–183. https://doi.org/10.1007/s10682-006-0021-0

González, F., & Pabón-Mora, N. (2017). Inflorescence and floral traits of the Colombian species of *Tristerix* (Loranthaceae) related to hummingbird pollination. *Anales del Jardin Botanico de Madrid*, *74*(2), e061. https://doi.org/10.3989/ajbm.2474

Guerra, T. J., Galetto, L., & Silva, W. R. (2014). Nectar secretion dynamic links pollinator behavior to consequences for plant reproductive success in the ornithophilous mistletoe *Psittacanthus robustus*. *Plant Biology*, *16*(5), 956–966. https://doi/10.1111/plb.12146

Hamrick, J. L., & Godt, M. J. W. (1997). Allozyme diversity in cultivated crops. *Crop Science*, *37*(1), 26–30. https://doi.org/10.2135/cropsci1997.0011183X003700010004x

Hardy, O. J., & Vekemans, X. (2002). SPAGEDI: a versatile computer program to analyse spatial genetic structure at the individual or population levels. *Molecular Ecology Notes*, *2*(4), 618–620. https://doi/10.1046/j.1471-8286.2002.00305.x

Hiscock, S. J., & McInnis, S. M. (2003). The diversity of self-incompatibility systems in flowering plants. *Plant Biology*, *5*(1), 23–32. https://doi.org/10.1055/s-2003-37981

Husband, B. C., & Schemske, D. W. (1996). Evolution of the magnitude and timing of inbreeding depression in plants. *Evolution*, *50*(1), 54–70. https://doi.org/10.2307/2410780

Jerome, C. A., & Ford, B. A. (2002). Comparative population structure and genetic diversity of *Arceuthobium americanum* (Viscaceae) and its *Pinus* host species: insight into host-parasite evolution in parasitic angiosperms. *Molecular Ecology*, *11*(3), 407–420. https://doi.org/10.1046/j.0962-1083.2002.01462.x

John, F. (1985). Explosive flower opening in ornithophily: a study of pollination mechanisms in some Central African Loranthaceae. *Botanical Journal of the Linnean Society*, *90*, 129–144. https://doi.org/10.1111/j.1095-8339.1985.tb02205.x

Jombart, T. (2008). adegenet: a R package for the multivariate analysis of genetic markers. *Bioinformatics*, *24*(11), 1403–1405. https://doi.org/10.1093/bioinformatics/btn129

Jombart, T., & Balloux, D. (2010). Discriminant analysis of principal components: a new method for the analysis of genetically structured populations. *BMC Genetics*, *11*, 94. https://doi.org/10.1186/1471-2156-11-94

Kirkup, D. W. (1998). Pollination mechanisms in African Loranthaceae. In: Polhill, R. M, &Weins, D.(Eds.), *Mistletoes of Africa*. London, UK: Kew Publishing.

Krauss, S. L., He, T., Barrett, L. G., Lamont, B. B., Enright, N. J., Miller, B. P., & Hanley, M. E. (2009). Contrasting impacts of pollen and seed dispersal on spatial genetic structure in the bird-pollinated *Banksia hookeriana*. *Heredity*, *102*(3), 274–285. https://doi.org/10.1038/hdy.2008.118

Ladley, J. J., & Kelly, D. (1995). Explosive New Zealand mistletoe. *Nature*, *378* (6559), 766. https://doi.org/10.1038/378766a0

Loiselle, B. A., Sork, V. L., Nason, J., & Graham, C. (1995). Spatial genetic structure of a tropical understory shrub, *Psychotria officinalis* (Rubiaceae). *American Journal of Botany*, *82*(11), 1420–1425. http://doi/10.1002/j.1537-2197.1995.tb12679.x

Luo, Y. H. (2012). Reproductive characteristics and ecological adaptability of *Dendrophthoe pentandra* (Master thesis), Graduate College of the Chinese Academy of Sciences.

Luo, Y., Sui, Y., Gan, J., & Zhang, L. (2016). Host compatibility interacts with seed dispersal to determine small-scale distribution of a mistletoe in Xishuangbanna, Southwest China. *Journal of Plant Ecology*, *9*(1), 77–86. https://doi.org/10.1093/jpe/rtv024

Martinez del Rio, C., Hourdequin, M., Silva, A., & Medel, R. (1995). The influence of cactus size and previous infection on bird deposition of mistletoe seeds. *Australian Journal of Ecology*, *20*(4), 571–576. https://doi.org/10.1111/j.1442-9993.1995.tb00577.x

Martinez del Rio, C., Silva, A., Medel, R., & Hourdequin, M. (1996). Seed dispersers as disease vectors: bird transmission of mistletoe seeds to plant hosts. *Ecology*, *77*(3), 912–921. https://doi.org/10.2307/2265511

Mathiasen, R. L., Nickrent, D. L., Shaw, D. C., & Watson, D. M. (2008). Mistletoes: pathology, systematics, ecology, and management. *Plant Disease*, *92*(7), 988–1006. https://doi.org/10.1094/pdis-92-7-0988

Mejnartowicz, L. (2006). Relationship and genetic diversity of mistletoe (*Viscum album* L.) subspecies. *Acta Societatis Botanicorum Poloniae*, *75*(1), 39–49. https://doi.org/10.5586/asbp.2006.007

Morrill, A., Dargent, F., & Forbes, M. R. (2017). Explaining parasite aggregation: More than one parasite species at a time. *International Journal for Parasitology*, *47*(4), 185–188. https://doi.org/10.1016/j.ijpara.2016.11.005

Ndagurwa, H. G. T., Mundy, P. J., Dube, J. S., & Mlambo, D. (2012). Patterns of mistletoe infection in four Acacia species in a semi-arid southern African savanna. *Journal of Tropical Ecology*, *28*, 523–526. https://doi.org/10.1017/s0266467412000387

Nei, M. (1978). Estimation of average heterozygosity and genetic distance from a small number of individuals. *Genetics*, *89*(3), 583–590.

Norton, D. A., & Ladley, J. J. (1998). Establishment and early growth of *Alepis flavida* in relation to *Nothofagus solandri* branch size. *New Zealand Journal of Botany*, *36*(2), 213–217. https://doi.org/10.1080/0028825X.1998.9512562

Nybom, H., & Bartish, I. V. (2000). Effects of life history traits and sampling strategies on genetic diversity estimates obtained with RAPD markers in plants. *Perspectives in Plant Ecology, Evolution and Systematics*, *3*(2), 93–114. https://doi.org/10.1078/1433-8319-00006

Overton, J. M. (1994). Dispersal and infection in mistletoe metapopulations. *Journal of Ecology*, *82*(4), 711–723. https://doi.org/10.2307/2261437

Peakall, R., & Smouse, P. E. (2012). Genalex 6.5: genetic analysis in Excel. Population genetic software for teaching and research-an update. *Bioinformatics*, *28*(19), 2537–2539. https://doi.org/10.1093/bioinformatics/bts460

Pérez-Crespo, M. J., Ornelas, J. F., Marten-Rodriguez, S., Gonzalez-Rodriguez, A., & Lara, C. (2016). Reproductive biology and nectar production of the Mexican endemic

Psittacanthus auriculatus (Loranthaceae), a hummingbird-pollinated mistletoe. *Plant Biology*, *18*(1), 73–83. https://doi.org/10.1111/plb.12365

Pettengill, J. B., & Moeller, D. A. (2012). Tempo and mode of mating system evolution between incipient *Clarkia* species. *Evolution*, *66*(4), 1210–1225. https://doi.org/10.1111/j.1558-5646.2011.01521.x

Potts, S. G., Biesmeijer, J. C., Kremen, C., Neumann, P., Schweiger, O., & Kunin, W. E. (2010). Global pollinator declines: trends, impacts and drivers. *Trends in Ecology & Evolution*, *25*(6), 345–353. https://doi.org/10.1016/j.tree.2010.01.007

Qiu, H. X., Gilbert, M. G. (2004). Loranthaceae. In: Wu, Z.Y., & Raven, P. H (Eds.), *Flora of China*, Vol. 5. Beijing, China: Science Press and Missouri Botanical Garden Press.

R Core Team. (2020). *R: a language and environment for statistical computing.* Vienna, Austria: R foundation for statistical computing. https://www.R-project.org/

Rist, L., Shaanker, R. U., & Ghazoul, J. (2011).The spatial distribution of mistletoe in a southern Indian tropical forest at multiple scales. *Biotropica*, *43*(1), 50–57. https://doi.org/10.1111/j.1744-7429.2010.00643.x

Ritland, K. (2002). Extensions of models for the estimation of mating systems using *n* independent loci. *Heredity*, *88*(4), 221–228. https://doi.org/10.1038/sj.hdy.6800029

Rodriguez-Riano, T. & Dafni, A. (2000). A new procedure to assess pollen viability. *Sexual Plant Reproduction*, *12*(4), 241–244. https://doi.org/10.1007/s004970050008

Sargent, S. (1995). Seed fate in a tropical mistletoe: the importance of host twig size. *Functional Ecology*, *9*(2), 197–204. https://doi.org/10.2307/2390565

Shirk, R. Y., & Hamrick, J. L. (2014). High but variable outcrossing rates in the invasive *Geranium carolinianum* (Geraniaceae). *American Journal of Botany*, *101*(7), 1200–1206. https://doi.org/10.3732/ajb.1400224

Skorka, P., & Wojcik, J. D. (2005). Population dynamics and social behavior of the Mistle Thrush *Turdus viscivorus* during winter. *Acta Ornithologica*, *40*(1), 35–42. https://doi.org/10.3161/068.040.0109

Smouse, P. E., & Peakall, R. (1999). Spatial autocorrelation analysis of individual multiallele and multilocus genetic structure. *Heredity*, *82*(5), 561–573. https://doi.org/10.1046/j.1365-2540.1999.00518.x

Smouse, P. E., Peakall, R., & Gonzales, E. (2008). A heterogeneity test for fine-scale genetic structure. *Molecular Ecology*, *17*(14), 3389–3400. http://doi/10.1111/j.1365-294X.2008.03839.x

Sreekar, R., Huang, G., Yasuda, M., Quan, R.-C., Goodale, E., Corlett, R. T., & Tomlinson, K. W. (2016). Effects of forests, roads and mistletoe on bird diversity in monoculture rubber plantations. *Scientific Reports*, *6*, 21822. https://doi.org/10.1038/srep21822

Stanton, S., Honnay, O., Jacquemyn, H., & Roldan-Ruiz, I. (2009). A comparison of the population genetic structure of parasitic *Viscum album* from two landscapes differing in degree of fragmentation. *Plant Systematics and Evolution*, *281*, 161–169. https://doi.org/10.1007/s00606-009-0198-0

Start, A. N. (2011). Some observations on an urban mistletoe *Dendrophthoe pentandra* (L.) Miq. (Loranthaceae) in Thailand. *Natural History Bulletin of the Siam Society*, *57*, 81–86.

Vekemans, X., Hardy, O.J. (2004). New insights from fine-scale spatial genetic structure

analyses in plant populations. *Molecular Ecology*, *13*(4), 921–935. https://doi.org/10.1046/j.1365-294X.2004.02076.x

Ward, M. J., & Paton, D. C. (2007). Predicting mistletoe seed shadow and patterns of seed rain from movements of the mistletoe bird, *Dicaeum hirundinaceum*. *Austral Ecology*, *32*(2), 113–121. https://doi.org/10.1111/j.1442-9993.2006.01668.x

Watson, D. M. (2020). Did mammals bring the first mistletoes into the treetops? *The American Naturalist*, *196*(6), 769–774. https://doi.org/10.1086/711396

Watson, D. M. (2001). Mistletoes - a keystone resource in forests and woodlands worldwide. *Annual Review of Ecology and Systematics*, *32*, 219–249. https://doi.org/10.1146/annurev.ecolsys.32.081501.114024

Weir, B. S., & Cockerham, C. C. (1984). Estimating F-statistics for the analysis of population structure. *Evolution*, *38*(6), 1358–1370. https://doi.org/10.2307/2408641

Weston, K. A., Chapman, H. M., Kelly, D., & Moltchanova, E. V. (2012). Dependence on sunbird pollination for fruit set in three West African montane mistletoes species. *Journal of Tropical Ecology*, *28*, 205–213. https://doi.org/10.1017/s026646741100068x

Xiao, L. Y., & Pu, Z. H. (1988). An exploration of the Loranthaceae in Xishuangbanna. *Acta Botanica Yunnanica*, *10*(1), 69–78. (In Chinese).

Yan, Z. (1993). Resistance to haustorial development of two mistletoes, *Amyema preissii* (Miq.) Tieghem *exocarpi* and *Lysiana exocarpi* (Behr.) Tieghem ssp *exocarpi* (Loranthaceae), on host and nonhost species. *International Journal of Plant Science*, *154*(3), 386–394. https://doi.org/10.1086/297120

Young, L. J., & Young, J. H. (1998). *Statistical ecology: a population perspective*. Boston: Kluwer Academic Publishers.

Yule, K. M., &Bronstein, J. L. (2018). Infrapopulation size and mate availability influence reproductive success of a parasitic plant. *Journal of Ecology*, *106*(5), 1972–1982. https://doi.org/10.1111/1365-2745.12946

Yule, K. M., Koop, J. A. H., Alexandre, N. M., Johnston, L. R., & Whiteman, N. K. (2016). Population structure of a vector-borne plant parasite. *Molecular Ecology*, *25*(14), 3332–3343. https://doi.org/10.1111/mec.13693

SUPPORTING INFORMATION

Methods for development of 13 microsatellite markers in *Dendrophthoe pentandra*

Genomic DNA was extracted from silica-gel-dried leaves by following the CTAB method and microsatellite loci were isolated by using fast isolation by AFLP of sequences containing repeats (FIASCO) protocol (Doyle & Doyle, 1987; Zane et al., 2002). Approximately 500 ng of total genomic DNA was digested with *Mse*I enzyme (New England Biolabs, Beberly, MA, USA) and then fragments were ligated to the *Mse*I AFLP adaptor pair (5'-

TACTCAGGACTCAT-3'/5'-GACGATGAGTCCTGAG-3') at 37 °C for 2 h with T4 DNA ligase (Fermentas, Burlington, ON, Canada). A diluted digestion-ligation mixture (1:10) was amplified with the adaptor-specific primers *Mse*I-N (5'-GATGAGTCCTGAGTAAN-3') by following the program: 95 °C for 3 min, 30 cycles of 94 °C for 30 s, 53 °C for 60 s, 72 °C for 60 s followed by an elongation step of 5 min at 72 °C. Amplified fragments with a size range of 200–800 bp were enriched for microsatellite repeats by magnetic bead selection with 5'-biotinylated $(AC)_{15}$, $(AG)_{15}$, and $(AAG)_{10}$ probes. Captured fragments were re-amplified with adaptor-specific primers. Polymerase chain reaction (PCR) products were purified by using an EZNA Gel Extraction Kit (Omega Bio-Tek, Guangzhou, China).

The purified PCR products with enriched microsatellite repeats were ligated into the pGEM-T vector (Promega, USA), and transformed into DH5α cells (TaKaRa, Dalian, China). Recombinant clones were screened by blue/white selection and the positive clones were tested by PCR with $(AC)_{10}$/$(AG)_{10}$/$(AAG)_7$ and T7/Sp6 primers. The clones with positive inserts were sequenced with an ABI PRISM 3730XL DNA sequencer (Applied Biosystems, Foster City, CA, USA). The program Oligo 6.0 was used to design locus-specific primers for those microsatellite sequences found to contain sufficient flanking regions (Offerman & Rychlik, 2003).

Polymorphisms of microsatellite loci were evaluated in 24 wild individuals of *D. pentandra* from three populations across Xishuangbanna (21°10'–22°40' N, 99°55'–101°50' E) southern Yunnan China. Polymerase chain reactions (PCR) were performed in 20 μL of reaction containing 30–50 ng genomic DNA, 0.6 μM of each primer, 7.5 μL 2 × *Taq* PCR MasterMix [Tiangen (Tiangen, Beijing China); 0.1 U *Taq* Polymerase/μL, 0.5 mM dNTP

each, 20 mM Tris-HCl (pH = 8.3), 100 mM KCl, 3 mM $MgCl_2$]. PCR amplifications were conducted under the following program: 95 °C for 3 min followed by 30–36 cycles at 94 °C for 30 s, with the annealing temperature optimized for each specific primer (Table S1) for 30 s, 72 °C for 60 s, and a final extension step at 72 °C for 7 min. The amplified fragments were separated on 6% polyacrylamide denaturing gels with a 20-bp ladder molecular size standard (Fermentas, Burlington, Ontario, Canada) by silver staining.

In total, 278 clones with positive inserts were sequenced with an ABI PRISM 3730XL DNA sequencer (Applied Biosystems Inc., USA). A total of 208 (75%) sequences were found to contain microsatellite repeats (SSRs), and 93 of them that have appropriate microsatellite and enough flanking regions were suitable for designing locus-specific primers, using the Oligo 6.0 program. Polymorphisms of all 93 microsatellite loci were identified with 24 individuals. Of these primers, 33 successfully amplified the target regions, and 13 of them displayed polymorphisms and six showed similar genetic diversity (see Table S1).

REFERENCES

Doyle, J. J., & Doyle, J. L. (1987). A rapid DNA isolation procedure for small quantities of fresh leaf tissue. *Phytochem Bull*, 19, 11–15.

Offerman, J., & Rychlik W. (2003). Oligo Primer Analysis Software. In S. Krawetz, and D. Womble [eds.], Introduction to Bioinformatics: A Theoretical and Practical Approach, 345–361. Humana Press, Totowa, USA.

Zane, L., Bargelloni, L., & Patarnello, T. (2010). Strategies for microsatellite isolation: a review. *Molecular Ecology, 11*(1),1–16. https://doi.org/10.1046/j.0962-1083.2001.01418.x

Table S1 Microsatellite loci analyzed in *Dendrophthoe pentandra*.

Locus	Primer sequences (5′-3′)	Repeat motif	Size (bp)	T_a (°C)	GenBank accession no.
DenP008	F: GCCATTTTGACTCCCTTTTT R: TTCTTTCTTGCTTGGCATCC	$(AG)_5ACTG(AG)_7$	216	52	KT264232
DenP023	F: ATAGGGAAAGTGAGCACAAA R: AATCAAGGCACAAAACAACG	$(AG)_{13}$	200	56	KT264233
DenP036	F: ATTCTAAACAATAACGACGA R: ATGACCACGTACACCGCCTG	$(AT)_5(GT)_6$	108	52	KT264234
DenP038	F: ACTTTGGGATGGTGGTTGTG R: TGTATTGTTAGGTGATTGGC	$(AC)_8$	111	52	KT264235
DenP043	F: TAGAAGGAGTGAGCGGAAGA R: GGAAGTTGAAGGCGAGAAA	$(TG)_7$	249	54	KT264236
DenP049	F: ATTAGAGTCAAAGTCACCGA R: GAGACAACCTGGATTCATAC	$(AC)_{10}AGAT(AG)_{12}$	154	58	KT264237
DenP058	F: ATGACAGTAGCGGGAGTGGA R: TTGGAGTGTTATAGGATGAA	$(TG)_9$	213	52	KT264238
DenP062	F: CGACATCACAGACCCAATCA R: AAGAACTTTTACACATACAC	$(TA)_5(TG)_8$	106	52	KT264239
DenP072	F: GATTGACAACCTTCGGGAGA R: TAAGAGTGCCGCTGGTAAAC	$(TC)_{11}$	224	57	KT264240
DenP080	F: GGAAATAAATAAAACGGAAT R: TACACACACTGACAAACACT	$(TG)_8$	117	50	KT264241
DenP083	F: CGAGGAGGGACTTTGGTTAT R: TGTCTCAATGCGAACACAAT	$(AC)_{15}$	199	52	KT264242
DenP084	F: TAGCCCGACAGTTAGAAATG R: TAGTTTGACCTTCCTGCTTA	$(AC)_9$	259	54	KT264243
DenP087	F: TGGGTTCTGACTCGCATCTC R: ATATGAACCCGACAATGGTC	$(TC)_6(AC)_7$	104	52	KT264244

Table S2 Statistic of binomial GLM: relationship between fruit set of mistletoe and several factors (populations, treatments, and interactions between populations and treatments), ***$P < 0.001$, **$P < 0.01$, *$P < 0.05$.

Model	Model formula	Parameter	Estimate	SE	Z	*P*	AIC
Model 1	Fruit set ~ treatment + population + treatment: population	Intercept	-3.6839	1.5685	-2.349	**0.019***	265.01
		Treatment_HC	3.1515	1.6323	1.931	0.054	
		Treatment_HG	2.3878	1.6396	1.456	0.145	
		Treatment_N	1.9074	1.6986	1.123	0.262	
		Treatment_S	2.1241	1.6874	1.259	0.208	
		Population_ML	-0.1003	1.9429	-0.052	0.959	
		Treatment_HC: Population_ML	-0.2441	2.0256	-0.121	0.904	
		Treatment_HG: Population_ML	-0.1373	2.0536	-0.067	0.947	
		Treatment_N: Population_ML	1.3009	2.0697	0.629	0.530	
		Treatment_S: Population_ML	1.7301	2.0658	0.837	0.402	
Model 2	Fruit set ~ treatment + population	Intercept	-4.1205	0.9564	-4.308	**< 0.001*****	270.85
		Treatment_HC	3.0252	0.9674	3.127	**0.002****	
		Treatment_HG	2.3956	0.9854	2.431	**0.015***	
		Treatment_N	2.8989	0.9619	3.014	**0.003****	
		Treatment_S	3.3908	0.9660	3.510	**< 0.001*****	
		Population_ML	0.5115	0.3099	1.651	0.099	

Table S3 Analysis of molecular variance (AMOVA) among populations, based on adult plants.

Source of variation	df	SS	EV	%
Among populations	3	171.381	1.424	32%
Among individuals	72	242.856	0.279	6%
Within individuals	76	214.000	2.816	62%
Total	151	628.370	4.803	100%

Note: df, degrees of freedom; SS, sums of squares; EV, estimate of variance component.

Table S4 Wright F-statistics estimated by AMOVA, based on adult plants in the four populations.

Fixation indices	Value	*P*-value
F_{ST}	0.315	0.001
F_{IS}	0.090	0.002
F_{IT}	0.377	0.001

Table S5 Estimates of parameters of a regression model of outcrossing rates in this study with the posterior probability (Pr) of ecological variables (Z). t = initial outcrossing rate. The HPD values in bold show the significant effects. b_0: constant, b_1: host tree height, b_2: tree crown volume, b_3: infection intensity, and b_4: mistletoe individuals per crown volume.

t	Locus	Parameter	Mean	HPD 95%	Pr (Z)
0.8	Multi	b_0	2.2032	1.8432; 2.6353	
		b_1	0	0	0.181
		b_2	-2.4028	-5.7872; 0.4741	0.734
		b_3	1.7989	-1.2289; 4.7611	0.591
		b_4	0	0	0.212
0.5	Multi	b_0	2.166	1.7577; 2.5632	
		b_1	0	0	0.15
		b_2	-0.6007	**-0.9161; -0.2754**	0.672
		b_3	0	0	0.501
		b_4	0	0	0.188
0.25	Multi	b_0	2.1975	1.8221; 2.6099	
		b_1	0	0	0.126
		b_2	-2.4598	-5.0124; 0.1491	0.7545
		b_3	1.8588	-0.2417; 4.7549	0.6115
		b_4	0	0	0.16
0.8	Single	b_0	1.4395	1.1471; 1.7257	
		b_1	0	0	0.131
		b_2	-2.3646	**-4.3414; -0.1617**	0.87
		b_3	1.8436	-0.254; 3.8885	0.552
		b_4	0	0	0.098
0.5	Single	b_0	1.4373	1.1598; 1.7479	
		b_1	0	0	0.154
		b_2	-2.5202	**-4.8203; -0.1897**	0.813
		b_3	2.0047	-0.2454; 4.3364	0.576
		b_4	0	0	0.103
0.25	Single	b_0	2.7466	2.2049; 3.2039	
		b_1	0	0	0.181
		b_2	-0.6487	**-1.0113; -0.2041**	0.734
		b_3	0	0	0.591
		b_4	0	0	0.212

Table S6 Posterior probabilities (Pr) of top two regression models (M) of each simulation. *t* = initial outcrossing rate. The model structure is shown as a binary code, denoting inclusion/exclusion of variables (0/1), ordered from the most probable model to the least. For example {1111} means all four variables namely, tree height (b_1), tree crown volume (b_2), infection intensity (b_3), and mistletoe individuals per crown volume (b_4) are presented in the model. See also Figure S3.

t	Locus	M	Structure	Pr(M)
0.8	Multi	6	{ 0110 }	0.2755
		2	{ 0100 }	0.273
0.5	Multi	2	{ 0100 }	0.341
		4	{ 0010 }	0.1995
0.25	Multi	6	{ 0110 }	0.314
		2	{ 0100 }	0.2735
0.8	Single	6	{ 0110 }	0.3855
		2	{ 0100 }	0.3535
0.5	Single	6	{ 0110 }	0.3665
		2	{ 0100 }	0.3115
0.25	Single	2	{ 0100 }	0.269
		4	{ 0010 }	0.261

Table S7 The observed parent-offspring incompatibility rates, mean mistyping error rates, allele dropout rates, and allele misclassification rates across MCMC for the single-locus scenario.

Loci	Parent-offspring incompatibility rates	Mean mistyping error rates across MCMC	Allele dropout rate for the l^{th} marker (e_1)	HPD 95%	Allele misclassification rate for the l^{th} marker (e_2)	HPD 95%
Loc_1:	0	0.0013 – 0.0045	0.0014	0 – 0.0068	0.0058	0.0017 – 0.0105
Loc_2:	0	0.0022 – 0.0032	0.0023	0 – 0.0112	0.0017	0 – 0.0052
Loc_3:	0	0.0027 – 0.0031	0.0021	0 – 0.0103	0.003	0 – 0.0068
Loc_4:	0.0024	0.0027 – 0.0044	0.0026	0 – 0.0127	0.0059	0.0015 – 0.0102
Loc_5:	0.0146	0.0013 – 0.0189	0.0012	0 – 0.0055	0.0173	0.0098 – 0.0248
Loc_6:	0.0012	0.0016 – 0.0028	0.0017	0 – 0.0064	0.0033	0 – 0.0072
Loc_7:	0.006	0.0007 – 0.0072	0.0008	0 – 0.0044	0.0092	0.0044 – 0.0152
Loc_8:	0	0.0012 – 0.0082	0.0018	0 – 0.0083	0.0058	0.0005 – 0.0114
Loc_9:	0.0122	0.0021 – 0.0114	0.0021	0 – 0.01	0.0131	0.0067 – 0.0192
Loc_10:	0	0.0014 – 0.0047	0.0014	0 – 0.007	0.007	0.0017 – 0.0127
Loc_11:	0.0092	0.0319 – 0.0123	0.0325	0.0034 – 0.059	0.0104	0.0052 – 0.0165
Loc_12:	0.0024	0.0005 – 0.0069	0.0005	0 – 0.0029	0.0068	0.0016 – 0.0116
Loc_13:	0.0012	0.0008 – 0.0024	0.001	0 – 0.0045	0.0035	0.0001 – 0.0071

Figure S1 Color changes of *Dendrophthoe pentandra* floral buds and flowers during anthesis.

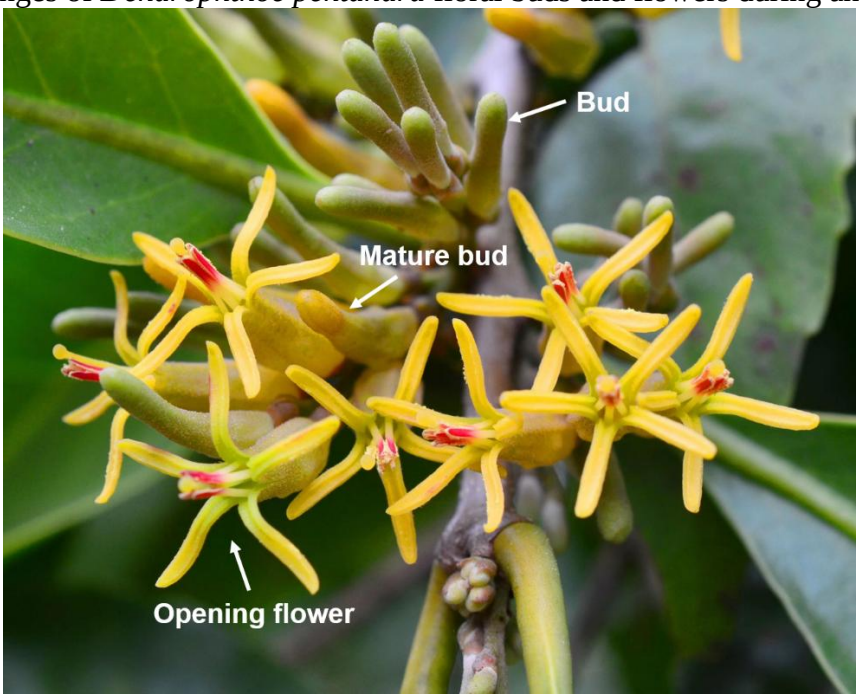

Photo credit: Dr. Renbin Zhu, Xishuangbanna Tropical Botanical Garden, Chinese Academy of Sciences.

Figure S2 Changes in pollen viability and frequency of stigma receptivity (A), and nectar secretion and sugar concentration dynamics (B) throughout flower anthesis of *Dendrophthoe pentandra* (mean ± SE).

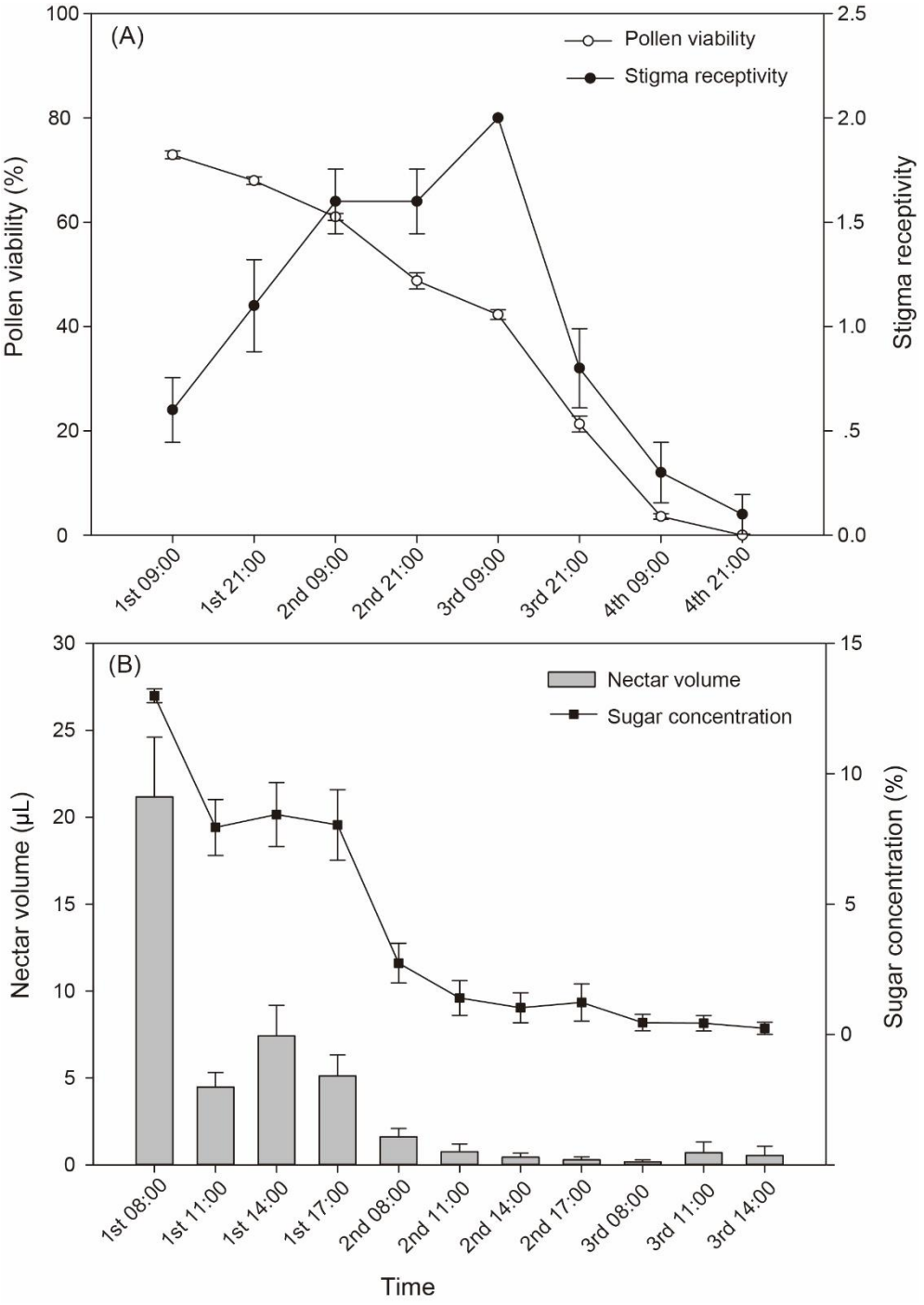

Figure S3 Regression model posterior probabilities for this study. The model structure is shown as a binary code, denoting inclusion/exclusion of variables (0/1), ordered from the most probable model to the least. The plot was truncated to show the ten most probable models (cumulative probability of ~0.95). For example {1111} means all four variables namely, tree height (b_1), tree crown volume (b_2), infection intensity (b_3), and mistletoe individuals per crown volume (b_4) are presented in the model.